Ejectable Data Recorder Module Engineered Design: A Component Bid for an Orbital Reentry Flight Test

A thesis submitted in partial fulfillment of the requirement
for the degree of Bachelor of Science in Physics from
The College of William and Mary

by

William Bushman

with

George Denny, Nathan McConnell, Aurora Santangelo, Rollin Woodford

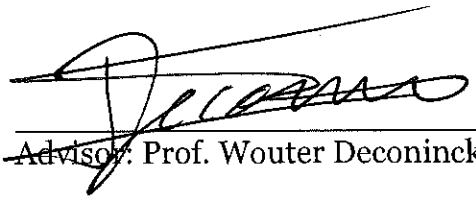

Advisor: Prof. Wouter Deconinck

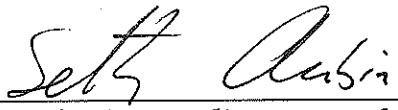

Senior Thesis Coordinator: Prof. Seth Aubin

Williamsburg, VA

May 3, 2019

Ejectable Data Recorder Module Engineered Design: A Component Bid for an Orbital Reentry Flight Test

A thesis submitted in partial fulfillment of the requirement
for the degree of Bachelor of Science in Physics from
The College of William and Mary

by

George Denny

with

Nathan McConnell, Aurora Santangelo, Rollin Woodford, William Bushman

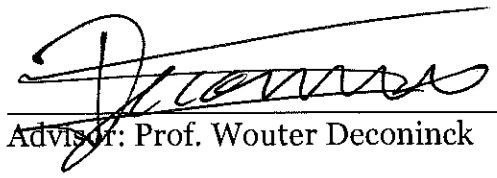

Advisor: Prof. Wouter Deconinck

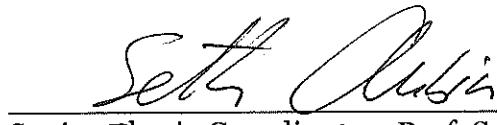

Senior Thesis Coordinator: Prof. Seth Aubin

Williamsburg, VA

May 3, 2019

Ejectable Data Recorder Module Engineered Design: A Component Bid for an Orbital Reentry Flight Test

A thesis submitted in partial fulfillment of the requirement
for the degree of Bachelor of Science in Physics from
The College of William and Mary

by

Nathan McConnell

with

Aurora Santangelo, Rollin Woodford, William Bushman, George Denny

Advisor: Prof. Wouter Deconinck

Senior Thesis Coordinator: Prof. Seth Aubin

Williamsburg, VA

May 3, 2019

Ejectable Data Recorder Module Engineered Design: A Component Bid for an Orbital Reentry Flight Test

A thesis submitted in partial fulfillment of the requirement
for the degree of Bachelor of Science in Physics from
The College of William and Mary

by

Aurora Santangelo

with

Rollin Woodford, William Bushman, George Denny, Nathan McConnell

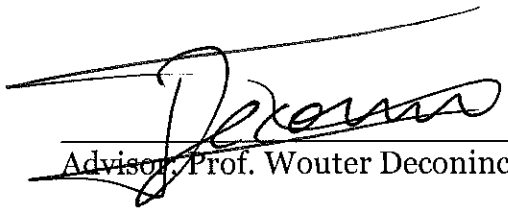

Advisor: Prof. Wouter Deconinck

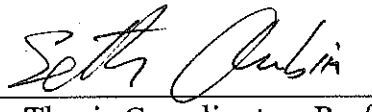

Senior Thesis Coordinator: Prof. Seth Aubin

Williamsburg, VA

May 3, 2019

Ejectable Data Recorder Module Engineered Design: A Component Bid for an Orbital Reentry Flight Test

A thesis submitted in partial fulfillment of the requirement
for the degree of Bachelor of Science in Physics from
The College of William and Mary

by

Rollin Woodford

with

William Bushman, George Denny, Nathan McConnell, Aurora Santangelo

Advisor: Prof. Wouter Deconinck

Senior Thesis Coordinator: Prof. Seth Aubin

Williamsburg, VA

May 3, 2019

Ejectable Data Recorder Module Engineered Design: A Component Bid for an Orbital Reentry Flight Test

A thesis submitted in partial fulfillment of
the requirement for the degree of Bachelor of Science in Physics
from the College of William & Mary in Virginia,

by

William Bushman, George R. Denny, Nathan J. McConnell,
Aurora B. Santangelo, Rollin Woodford

Advisor: Prof. Wouter Deconinck

Senior Thesis Coordinator: Prof. Seth Aubin

Williamsburg, Virginia
May 2019

Contents

Acknowledgments

We would like to thank our advisors, Prof. Wouter Deconinck, Carrie Rhoades, and Adam Beck, as well as the following people for their help and counsel to us during our year of research. Our contacts have included William & Mary faculty and staff, and leaders in the engineering industry. We could never have come this far and learned so much without the help of everyone listed, and many more. We are very grateful to have had the opportunity to have worked with all of you.

Prof. William Cooke ..... W&M Physics
Stewart Davis ..... CRP Technologies, USA
Robert Dillman ..... NASA LaRC
Jonathan Frey ..... W&M Physics
Prof. Donglai Gong ..... VIMS Physical Sciences
Jim Gray ..... Green Stream Technologies, Inc.
William Henninger ..... W&M Physics
Walter Holemans ..... Planetary Systems Corp.
Jeanna Hudson ..... VIMS Physical Sciences
Marty Manno ..... Diab
Jason McDevitt ..... W&M Technology Transfer
Thom Murray ..... Engineered Syntactic Systems

Lawrence "Bird" Taylor ..... NASA LaRC

David Williard ..... W&M Multimedia News

List of Figures

List of Tables

Abstract

The Ejectable Data Recorder (EDR) is a custom designed satellite component intended for NASA Langley Research Center (LaRC) flight tests of the Hypersonic Inflatable Aerodynamic Decelerator (HIAD), a technology demonstration mission for upcoming crewed Mars missions. Our EDR module is designed for low-earth-orbit and oceanic environments, and satisfies mass, volume, and impact constraints dictated by the HIAD flight test mission directors. It is designed to be easily retrievable post-flight-test, to provide redundancy in deceleration data recording, in the event that the primary payload of the HIAD is unable to be recovered. Our team is operating under Agile methodology for engineering design team organization, and making new strides with it by applying it to hardware development in educational environments.

Chapter 1

Introduction

1.1 The EDR Project

When sending spacecraft to other celestial bodies, a principal challenge for the mission controllers is landing the craft safely. Not only must it be oriented properly for descent, but any spacecraft must decelerate heavily before reaching the surface if it is to land intact. For moons and planets with an atmosphere, such as Titan, Venus, and Mars, the most mass-efficient way to decelerate an object is to take advantage of atmospheric drag as the craft enters the atmosphere. Historically, this method has always provided a soft limit on the available landing locations – because it takes time for the atmosphere's drag to decelerate a spacecraft, the craft could not slow down adequately to safely land at higher altitude locations. Furthermore, the entry speed of spacecraft increases with its mass, meaning that it would take longer for larger payloads to reach a maximum safe speed (too long to land them at all beyond a certain mass threshold).

A new technology being developed by NASA seeks to change this dilemma. It is the HIAD, or Hypersonic Inflatable Aerodynamic Decelerator (Figure 1.1). The HIAD is essentially a massive sail that can be implemented into spacecraft, stored away when they launch from Earth, that will inflate and expand out as the craft

approaches its destination to provide an enormous surface for atmospheric drag to push against as it begins its descent. The HIAD serves as an enormous "brake" on the craft, allowing it to begin decelerating from higher up in the atmosphere and to decelerate more rapidly. This will allow for payloads to reach their maximum safe landing velocity sooner and thus be sent to higher altitude landing locations. Additionally, by providing greater overall drag the HIAD will allow for more massive payloads to be landed safely.

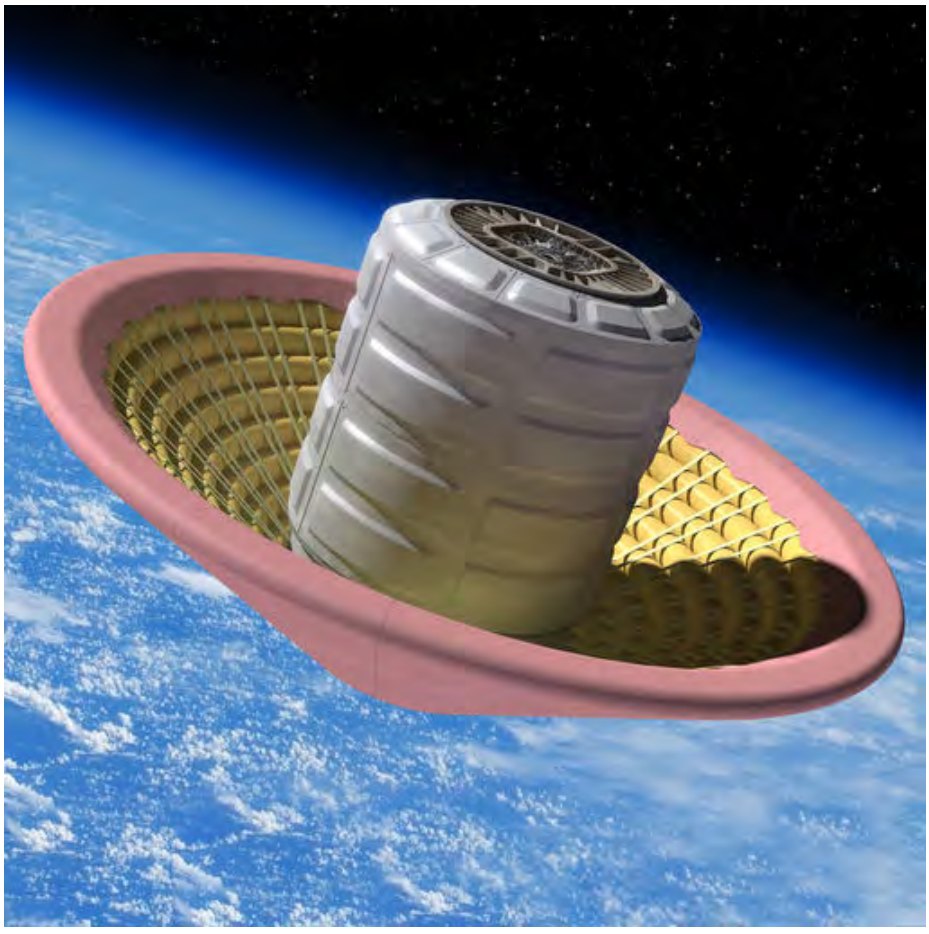

Figure 1.1: A conceptual drawing of NASA's Hypersonic Inflatable Aerodynamic Decelerator (HIAD), in development for manned missions to Mars. The EDR will record flight data aboard the HIAD during on-Earth testing. Figure from NASA website for HIAD.

The HIAD technology is still in development by NASA, with a flight test of a

six-meter diameter HIAD device planned for late 2021 or early 2022. To test the HIAD, it will be sent up into Low-Earth Orbit and then dropped back down into Earth's oceans, inflating out and coming down through Earth's comparatively dense atmosphere. This will allow scientists and engineers to see how well it performs its function in a known environment.

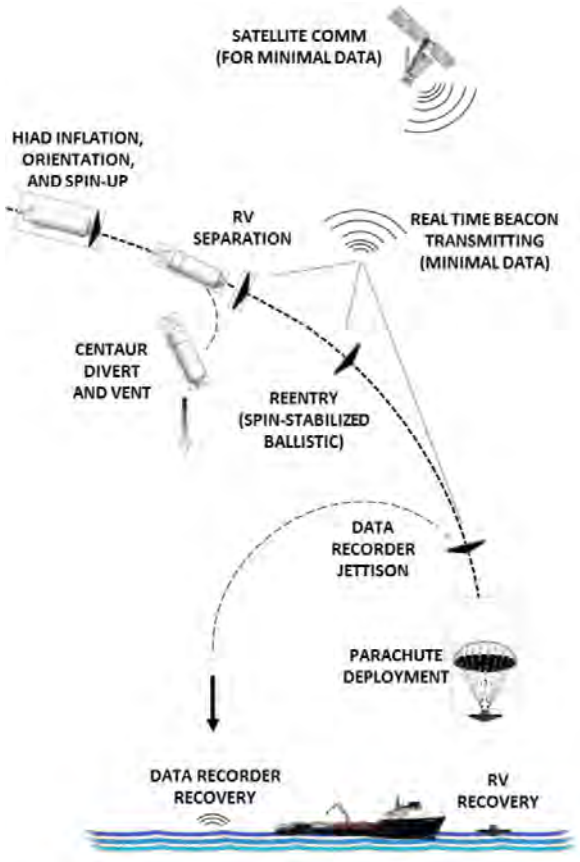

Figure 1.2: Diagram of the latter end of the HIAD Flight Test, in which the EDR is active. The EDR sends data in real time during orbital reentry, and is ejected from the HIAD at 50,000 ft above sea level. Recovery of the HIAD will be attempted immediately, but the EDR must await a recovery team for up to thirty days post-flight. Figure adapted from Carrie Rhoades.

Our project has been working to design an Ejectable Data Recorder, known as the EDR, for use with such tests of the HIAD device. Similar tests performed previously

by NASA, such as the IRVe tests, have resulted in the loss of the primary payload and with it, all of the flight data gathered during the test. The EDR will be a small shell which holds the flight data from a HIAD test and ejects out from the main payload during re-entry. It is meant to serve as a "black box" for future HIAD tests and is designed to safely land in the ocean and retain stable flotation for up to thirty days while awaiting recovery by NASA. Previous tests by NASA have made use of ejectable data recorders, such as the AA-2 test. However, our group is designing this EDR specifically for use with the HIAD payload. The EDR should ideally guarantee flight data recovery for future tests of HIAD devices.

1.2 HIAD Mission Scope

While our EDR design is intended only for flight tests of a HIAD in 2021 or 2022, the overall context of what comprises a HIAD system as well as understanding its goals are crucial. In past missions, a wide variety of factors limit what, how much, and how often spacecraft are sent to other planets. We are currently approaching a new throttling factor: logistics of mass and maximum capacity for entry, descent, and landing technologies. Over the past four decades, surface missions to Mars have included increasingly ambitious masses, ranging from the 600 kg of the first Viking landers to the metric ton of Curiosity. However, if NASA or members of the space industry wish to propel the exploration of Mars forward and entertain the possibility of human missions, then much more mass needs to be sent to the surface. Conservative estimates for short duration human missions (approximately 30 sols) recommend 20 metric tons of supplies for habitats, consumables, and auxiliary systems. In order to reach these drastically higher mass requirements, new technologies and techniques must be developed. The HIAD design uses the compact expandable nature of inflatables to send a large scale decelerator to enable ambitious planetary missions with

high mass payloads.

Before a HIAD lands mass on any planetary surface, researchers at LaRC and other centers put their design through rigorous testing. While contractors assembled rudimentary inflating tubes and composite textile sheaths, they took meticulous care to ensure that the forces, pressures, and shears internal and external to the HIAD are accommodated. Once contractors conclude that their design met the requirements given by LaRC, the inflatable design was applied after being launched to the edge of the atmosphere on a sounding rocket. NASA has performed three Inflatable Reentry Vehicle Experiments (IRVE 1 - IRVE 3) to determine how much drag the design could generate, and compare this physical data to models of expected performance. After reevaluating design choices at every opportunity to iterate possibilities and analyze performance, LaRC is now investigating a new test for a HIAD. Current plans are to enter the atmosphere from a low-Earth orbiting trajectory (LEO). As NASA prepares for a flight test from LEO to the surface to gather reentry data, we are designing our EDR to fit into the concept of operations of this type of mission.

While the precise details of the full-scale flight plan are not definite, we have some specifics to work from. A HIAD will be launched into LEO to orbit for multiple hours but less than a day, then will begin its reentry. As this occurs, sensors will record information such as temperature, pressure, gradients of the aforementioned measurables across the surface, as well as take videos in both visual light and infrared spectrum. Our EDR will record these observations to physical memory as SD cards. Then, after atmospheric reentry, at 50,000 feet altitude, our recorder will eject. By separating from the HIAD, the experimental information is preserved and decoupled from performance of the test platform. If chosen as a final component, our EDR will improve redundancy of the data collection and help to ensure that vital details will be preserved regardless of the fate of the HIAD test platform.

Separation from the HIAD presents our team with subtle but essential design elements. While we must account for the various environments our recorder will survive in, the transition between the orbital stage of the mission to the buoyant stage of the mission is not as complex as it may seem. Since the EDR will eject at 50,000 feet (and is collecting data on the heating during descent and ejecting after the period of interest has passed) the design is simplified considerably. Jettisoning from the reentry vehicle in the stratosphere is past the point at which significant heating occurs during reentry. Thus, beyond choosing materials that are acceptable both in aerospace and pelagic use, our limiting factor in design is reduced to the external forces acting on the EDR. The concept of operations of the HIAD flight test simplifies our design to planning for the few variables that will affect our EDR, namely the impact force imparted to it when it lands in the ocean and the marine environment it will remain exposed to for the duration of the mission.

1.3 Product Requirements

1.3.1 Volume

NASA required that we keep our EDR within a 4 inch square size constraint. While the EDR could be smaller than this and does not have to be any specific shape, it could not exceed the constraint.

While we could make the EDR any size and shape up to the 4 inch square constraint we were given, it made the most sense for us to us as much of the 4 inch plane perpendicular to the vertical axis, so that we could have the largest surface area possible directed towards the direction of descent, to increase the coefficient of drag, and slow descent. Also, it was logical to take advantage of the rest of the allowed volume, as it would give us the most room to store components and ballast inside the shell shape we would go on to create.

The reason for the 4 inch square volume constraint was that the EDR has to fit inside the HIAD's payload ejection device. This device sits at an angle inside the HIAD and will shoot out the EDR during the return back into the atmosphere. If the EDR we design is larger than the payload ejection device then it will of course not be usable.

1.3.2 Mass

NASA required that the EDR we designed could not exceed two pounds mass. As with the volume requirement we could have the EDR be lighter than this constraint but not higher.

Again as with the volume constraint, it was logical for us to use as much of the mass constraint as possible. In our design, we want the EDR to fall without tumbling. As well as designing the EDR to have the aerodynamics to correct itself and fall uniformly on descent, we can also take advantage of the leftover mass available, after filling the shell shape we designed with the appropriate electronics and potting, by filling the tip of the leading face on descent, with a high-density mass such as tungsten.

The reason for this mass requirement is that putting mass in space is very expensive. It costs roughly $10,000 USD for every pound that goes into space. If we exceeded the two pounds mass limit, it would cost that much more to put the payload in space.

1.3.3 Low-Earth Orbit

NASA required that our EDR be able to withstand the temperature extremes of Low-Earth Orbit for approximately eight hours.

This requirement presented a fairly difficult problem to solve. Many of the foams and potting material we were hoping to use inside the shell were not possible to use in

the vacuum conditions found in Low-Earth Orbit. If we used one of these materials, the volume of the foam would change while in orbit, potentially expanding beyond our volume bounds of 4 inch by 4 inch by 4 inch, and possibly affecting the shell such that it would not be watertight when it impacted the water.

We were able to find potting material that would not change its size while in orbit. Engineered Syntactic Systems has a Syntactic Foam that fits our needs for both the orbit and water environments that the EDR will experience.

1.3.4 Ejection and Water Impact

NASA required that our EDR be able to withstand the ejections force of the HIAD's payload ejection device of approximately 1,525 lbf, as well as being able to withstand a water impact from 50,000 feet.

The high ejection force the EDR will have to experience is due to the fact that the payload needs to be launched far enough and hard enough away from the HIAD to be able to escape the air distortion that the flight of the HIAD causes. If the payload is not launched far enough, it could get caught up in the HIAD and could compromise the survivability of both the EDR and the HIAD.

The EDR has to be able to withstand the force experienced from the 50,000 foot drop at terminal velocity as it impacts the water, because if it does not, the data stored on the electronics inside the shell shape will be lost. If the shell shape breaks on impact, the buoyancy of the shell shape will be compromised and it will sink, or water will get into the electronics and possibly destroy the stored data.

1.3.5 Seaworthiness

NASA required that our EDR be able to survive for 30 days in salt-water conditions, such as those found in the Pacific or Atlantic Ocean.

This means that not only does the EDR have to be able to stay afloat for those 30 days, but it also has to be water tight. This was achieved by using the potting previously mentioned, as well as using a material called Wind-form for the shell of the EDR.

Through testing done at VIMS we found that the Wind-form material would not significantly degrade while submerged in salt-water for an extended period of time. This will keep water from seeping in to the potting and electronics inside the shell, and keep the stored data safe.

1.3.6 Recovery

NASA required that our EDR be able to be located and recovered after its maximum 30 days in the ocean.

For it to be logical for us to use any kind of high-visibility device on top of the EDR, we need it to stay upright in the water, so that both the High-Visibility device can be seen, the GPS can be communicated with, and the solar panels can be powered by sunlight.

To keep the EDR upright we weighted the EDR with a high density mass in the bottom of the descent face. Not only does this keep the EDR from tumbling during descent, but it also keeps the EDR upright while in the water.

1.4 Agile Methodology

It was required by Carrie Rhoades that the EDR project be structured according to Agile methodology for team design. Agile is emerging as the most productive and efficient methodology for any design project to follow, from small teams such as this one to huge enterprises, like IBM and Microsoft. Some anticipate that government agencies such as NASA should convert to Agile development as well, to keep pace with

private Agile companies. It is Rhoades' hope that our work on this project through Agile should demonstrate the methodology's compatibility with the engineering design standards of NASA.

Agile has many variants intended for differing team dynamics and design methods. At its most general application, Agile is an umbrella term representing a set of practices which allow a team to work at a fast and iterative pace [3]. It enables a team to react immediately to any change in product requirements or industry standards.

Traditional planning would involve a definitive development schedule plotted against one final product deadline. Any time spent planning the design timeline is time taken away from actually developing the product. With modern industry technology and immediate customer feedback, product requirements could change at any point in the development process. A design team which has invested significant time, labor, and money into its only product development schedule will fall behind, with its design left obsolete.

Agile salvages time wasted in planning by setting short, intermediate deadlines well before the desired completion date. A product due in a year might have deadlines broken down to every week, and in each week, the design team prioritizes tasks based on what is immediately necessary and currently feasible at that stage of development.

In this way, the fundamental structure of Agile is cyclical, repeating at every short deadline, in the form of a "Sprint" (Figure 1.3). In a full-time design team, the length of a Sprint is traditionally one to two weeks. As a team of students, we have extended Sprints to three weeks. Each Sprint is brought to a close with a Demonstration to the product owners, followed by a team Retrospection, and then task Planning for the next Sprint.

The task-based Sprint structure keeps work flow constant. It mandates open communication between the design team and the product owner, or the client. The

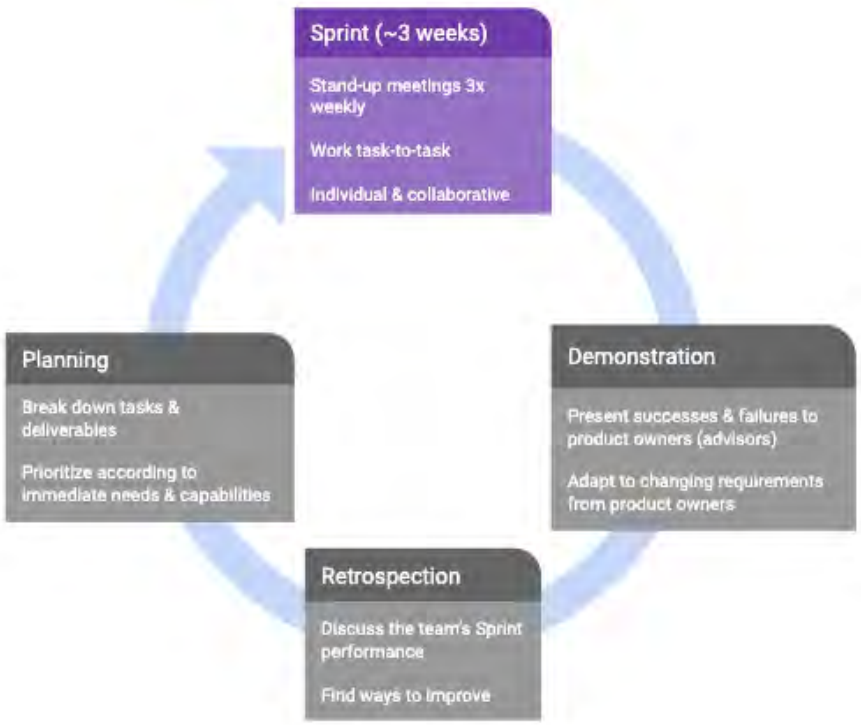

Figure 1.3: The Agile Sprint cycle, adapted to this student research project. Most of the cycle is dedicated to a 3 week Sprint. The 3 gray tiles ideally take place on the same day. Every Sprint ends in a Demonstration, or presentation, for the product owners (advisors, in our case), immediately followed by a group Retrospection of the team's performance. The team then holds a meeting to plan the next Sprint, in which we identify and prioritize tasks according to immediate needs and capabilities.

benefit of this close relationship is twofold: it allows for the product owners to relay changes in the product requirements to the design team at any time, and in turn, the design team can approach the product owners immediately when faced with something that stops development progress.

In addition to perfect group communication, Agile requires that the individual be committed to ultimate efficiency and accelerated quality assurance as well. Effective use of Agile requires a complete understanding and commitment to its principles. On both the interpersonal and individual level, such an understanding takes time,

Task Rating	Time or Significance
1	1 day or less, perhaps trivial
2	More than 1 day
3	Until the next standup
5	1 week, 3 standups
8	Too long, must be broken into smaller tasks

Table 1.1: Relative time rating in days used to characterize tasks during Sprint Planning, traditionally scaled by the Fibonacci sequence. A rating of 8 or higher is never used in this project. Such a task would take more than 1/3 of a Sprint to complete, and therefore must be broken down into smaller tasks before Sprint Planning is closed.

training, and practice.

The EDR team has been guided in Agile methodology by our mentor, Adam Beck, a business Agility coach and DevOps specialist who consults with Carrie Rhoades in projects at LaRC. He has been training us in the Spring semester for certification in Scaled Agile Framework (SAFe) for Lean Enterprises. SAFe is designed to accommodate large-scale, multi-tier operations, but is applicable to single-team projects as well. At the smallest scale, the applied flavor of Agile is Scrum, which operates much like our own adapted Sprint cycle process, as shown in Figure 1.3.

In a typical application of Agile, the project is software-based, and members of the team work on the project full time. We, however, are applying Agile to hardware development, and in a student setting. Given the time each member of the team dedicates to the project amidst courses, assignments, and outside work, we as a team of five operate approximately as one person would in a 40-hour work schedule.

In our 3-week Sprints, we host Standup meetings every Monday, Wednesday and Friday, and tasks are broken up such that most are possible to complete between Standups. At each Planning session before a Sprint, we rate tasks according to the projected time they are expected to take, scaled by days in a Fibonacci sequence

Sprint	Dates [Planning - Demo]	Duration	Agile "Velocity"	Description/Focus
1	5 - 30 Sep. 2018	3.5 weeks	(Not rated)	Product requirements & preliminary shell designs.
2	1 - 19 Oct. 2018	3 weeks	41	First conversations with VIMS, shell designs, physical materials, terminal velocity, parachute.
3	22 Oct. - 16 Nov. 2018	4 weeks	43	Qualitative shell aerodynamics test, terminal velocity, force of impact, outer shell materials/Windform, electronics survivability, SRL testing begun.
4	19 Nov. - 7 Dec. 2018	3 weeks	15	Mid-year COLL 400 presentation. Semester in review, electronics on impact, damped oscillation shell float test, weighted force of impact drop test.
5	10 Dec. 2018 - 21 Jan. 2019	6 weeks	12	Winter break, no Demo. Electronic components research by individual team members.
6	21 Jan. - 8 Feb. 2019	3 weeks	18	Wired Sandbox drop test, SRL update, future experiment planning.
7	11 Feb. - 1 Mar. 2019	3 weeks	30	Wireless Sandbox drop test, 1st lateral launch slo-mo test, syntactic foams, explored shell fairings for drag.
8	4 - 29 Mar. 2019	4 weeks	27	Included 1-week Spring break. 2nd lateral launch slo-mo test, GPS/radio electronics & code.
9	1 - 25 Apr. 2019	4 weeks	41	Final COLL 400 presentation. Year in review, demonstration launch of an assembled EDR.

Table 1.2: Timeline of Sprints from the beginning of the project until its projected conclusion at the final COLL 400 presentation. Agile "velocity" of each Sprint is measured in points (rated tasks) completed.

(Table 1.1). Most tasks should be rated at one to three days (or points). Any task rated at an eight or higher must be broken down into sub-tasks before Sprint Planning is complete. We used an online list-making application to create shared collections of tasks for each Sprint, sorted into the categories "To Do," "In Progress," "Done," and "Hold" (Figure 1.4).

Rating tasks during Sprint Planning allows the team to quantitatively and realistically predict the amount of work that can be done in the time of the next Sprint. At every Sprint's end, the team also sums up the points completed, to give the Sprint a "velocity."

In this year of research, we have completed nine Sprints, with velocities that vary according to mid-year breaks and heavy waves of exams in other courses (Table 1.2). We have grown more confident in estimating the work load for every Sprint, working

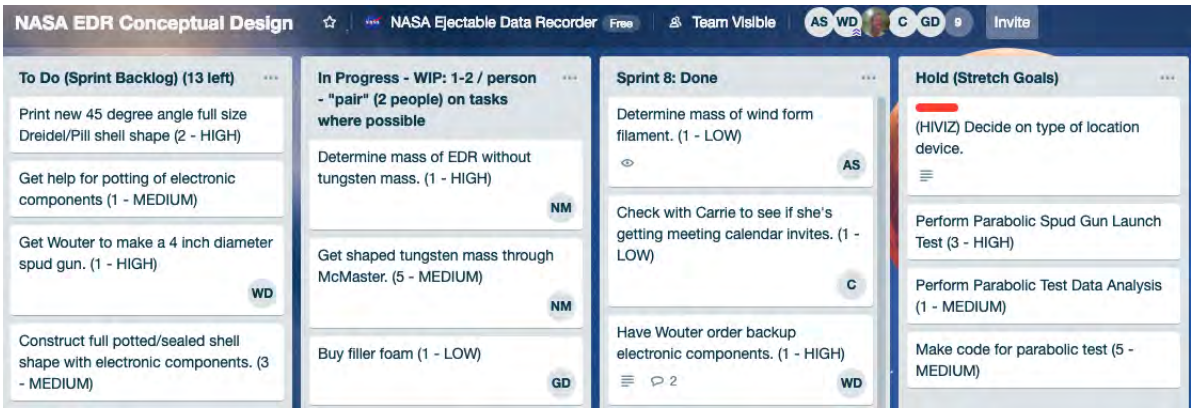

Figure 1.4: A sample screenshot of our Trello board, a shared list of running Sprint tasks.

around exams and school breaks. We have also benefited from the extensive documentation that Agile has required of us. Between Scribe notes from every Standup, slides from regular, summarizing Demonstrations, Trello boards, shared documents, and our website, the progress of this year of research is exceedingly well documented.

Chapter 2

Theory

2.1 Terminal Velocity

In developing an EDR meant to successfully make a round trip from orbit back down to the Earth, survivability is a chief concern of the development process. As such, the return fall is arguably one of the most important factors to take into consideration. In tandem with the impact force, the speed at which the object falls is a determining factor in just how much force will be imparted. In particular, the maximum velocity an object can possibly reach in a medium, known generally as "terminal velocity" is a useful calculation to the mission.

In understanding terminal velocity, one must first be aware of the concept of drag. In accordance with standard fluid dynamics, when an object is moving through a medium, it exerts a force on the atoms of the medium as it maintains its motion. As a result, this causes a stagnation pressure in the contents of the medium, and it begins to exert a slowing force in the opposite direction, known as drag. The phenomenon of drag is dictated by several factors, many of which change with time and position consistently. The equation for how much drag force F_D is applied to an object is as follows:

$$F_D = \frac{1}{2}\rho v^2 C_D A \tag{2.1}$$

where ρ refers to the density of the fluid, v refers to the velocity of the object through the fluid, A is the cross-sectional area of the object, and C_D is what is known as the coefficient of drag. As expressed in the equation, drag force is directly proportional to the speed and cross-sectional area of an object. That is to say that the faster an object moves or the larger it is, the more force will be created as a result.

The coefficient of drag is a dimensionless quantity that is used to quantify the amount of drag a given object will experience in all mediums. The value is roughly determined by the shape of the object in question, with lower coefficients of drag corresponding to lower drag force, or more aerodynamic or hydrodynamic movement. This coefficient is the only part of the drag function not readily obtainable by simple measurement or calculation, and as such has been sought out as an element to keep track of for each of the designs we have developed.

The terminal velocity v_t of a falling object is the velocity at which the drag force upwards is equal to the force due to gravity, mg (where m is the mass of the object and g is the acceleration due to gravity). As a result, the acceleration of the object becomes zero, and the object will no longer change its speed (provided the other conditions remain constant). Terminal velocity is of course a calculation of a maximum limit, which in physical reality is never truly reached, but rather is asymptotically approached. A formula for the terminal velocity can easily be obtained via simple algebra:

$$mg = \frac{1}{2}\rho v_t^2 C_D A \tag{2.2}$$

$$v_t = \sqrt{\frac{2mg}{\rho C_D A}} \tag{2.3}$$

A lower drag force implies a higher terminal velocity and vice versa. In a true Earth model, ρ and g both increase with proximity to the surface, affecting the

terminal velocity calculation by adding to its computational complexity.

It is important to determine the terminal velocity of our EDR for a couple of reasons. The first most obvious reason is that the higher the terminal velocity, the higher the impact force upon touchdown will be, and that is something that needs to be accounted for in the survivability of the design. For example, being able to survive an impact force from terminal velocity is the main point of contention as to whether or not a parachute is necessary. To that effect, knowing the height at which terminal velocity is reached and the percentage of terminal velocity reached by a certain height is useful to know for preliminary drop tests. Naturally it is unfeasible to perform a simple drop test from the desired 50,000ft, but a few hundred foot drop for instance would be much more manageable as a test.

C_d	Mass (kg)	Gravity	F_g	Surface Area m^2	Air Density (sea level)	V_t	Time of Impact
0.5	0.907	9.81	8.89767	0.01	1.225	53.90140659	0.1
Time	Acceleration m/s2	Velocity m/s	Position m	F_d		% of V_t	Impact Force (N)
0	-9.81	0	0	0		0	0
0.2	-9.81	-1.962	-0.5886	0.01178892225		0.03639979221	-17.79534
0.4	-9.797002291	-3.924	-1.569340046	0.047155689		0.07279958443	-35.59068
0.6	-9.758009163	-5.883400458	-2.941180321	0.1060066029		0.1091511489	-53.36244216
0.8	-9.693123922	-7.835002291	-4.702043257	0.1879984865		0.1453580303	-71.06347078
1	-9.602724932	-9.773627075	-6.848823171	0.2925415953		0.1813241563	-88.64679757
1.2	-9.487462409	-11.69417206	-9.377406831	0.4188080844		0.2169548589	-106.0661406
1.4	-9.34824908	-13.59166454	-12.28270472	0.5657458692		0.2521578824	-123.2763974
1.6	-9.186244907	-15.46131436	-15.55869249	0.7320974903		0.2868443578	-140.2341212
1.8	-9.002836284	-17.29856334	-19.19846189	0.9164233993		0.3209297203	-156.8979695
2	-8.799610365	-19.0991306	-23.19428021	1.117128918		0.354334549	-173.2291145
2.2	-8.578325338	-20.85905267	-27.53765725	1.33249399		0.3869853124	-189.1916077
2.4	-8.34087763	-22.57471774	-32.21941835	1.56070476		0.4188150025	-204.7526899
2.6	-8.089267078	-24.24289326	-37.22978235	1.799885989		0.4497636481	-219.8830419
2.8	-7.825561203	-25.86074668	-42.55844291	2.048133295		0.4797786981	-234.5569724
3	-7.551859653	-27.42585892	-48.19465189	2.303544321		0.5088152732	-248.7525404
3.2	-7.270259844	-28.93623085	-54.12730325	2.564247959		0.5368362846	-262.4516138
3.4	-6.982824742	-30.39028282	-60.34501631	2.82843095		0.5638124261	-275.6398652
3.6	-6.691553528	-31.78684777	-66.83621694	3.094361304		0.5897220458	-288.3067093
3.8	-6.398355784	-33.12515847	-73.58921575	3.360408129		0.61455091	-300.4451874
4	-6.105029626	-34.40482963	-80.59228226	3.625057675		0.6382918704	-312.0518048
4.2	-5.813244019	-35.62583556	-87.83371426	3.886925487		0.6609444504	-323.1263285
4.4	-5.524525373	-36.78848436	-95.30190164	4.144764781		0.6825143662	-333.6715531
4.6	-5.240248312	-37.89338943	-102.9853845	4.397471199		0.7030129978	-343.6930422

Figure 2.1: Excerpt of the dynamic table used to calculate terminal velocity with drag coefficients and physical parameters changeable to our needs.

In order to complete preliminary calculations of the possible terminal velocities prior to having a shape decided on, a dynamic table was created to account for all possibilities (Figure 2.1). Using time step calculations, the acceleration, velocity, and position of the EDR were calculated using standard kinematics. A number of placeholder assumptions are utilized in the above figure, namely the mass and surface area, estimated as the max possible for our requirements, and the force of gravity and air density which, for the sake of preliminary testing, are assumed to be those of sea level.

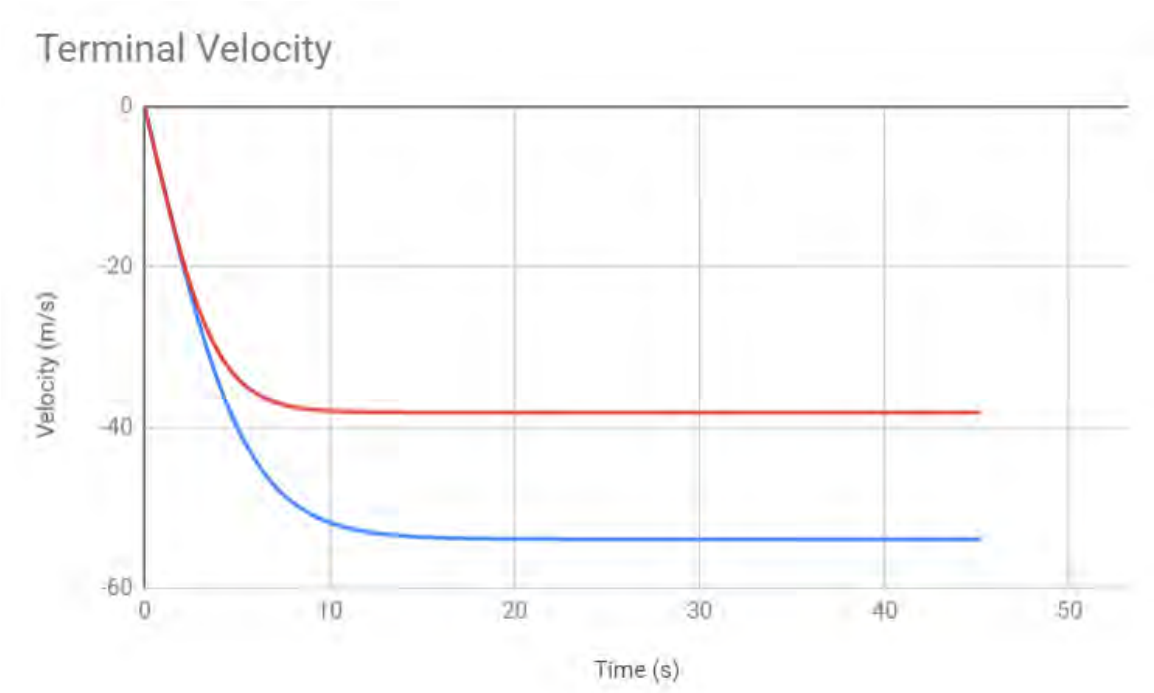

Figure 2.2: Graph derived from the dynamic table in Figure 2.1. It plots velocity as a function of time with drag coefficients of .5(blue) and 1.0(red). Terminal velocity is clearly shown to be approached asymptotically.

Due to the small size of our EDR, in conformance with our constraints, the calculations show that 90% of terminal velocity for all coefficients of drag is reached within the first 8 seconds of descent, at descent distances ranging between 100 and

300 meters.

The final shape that was chosen, which will be explained in detail in the following sections, has a 37.5^o angle cone as its downward facing surface. Final values for the terminal velocity of an object with the profile of a cone, known to have a coefficient of drag estimated to 0.5, giving it an estimated terminal velocity of 53 m/s.

2.2 Distribution of Mass & Mass Budget

One of the limitations placed on our design by the mission specifications is that the EDR must have a maximum weight of two pounds, or just under a kilogram of mass. However, this is not actually the final mass budget of the EDR. Instead, we know that our product must float in saltwater, meaning that its mass in the water can only be as much as the mass of the water that it displaces. This has forced us to consider what exactly we can include in our design, as well as how to arrange the parts that we do include inside. One thing that has become apparent in our work is that the material we choose to build the EDR out of, as well as its volume and density, constrains our mass budget quite significantly. Some materials are of course denser than others (ABS being the most frequent one we used and among the lightest), the shell itself has a variable mass. To handle this ever changing set of variables, we built a calculator in Colaboratory, a Python 3 Integrated Development Environment (IDE) that functions within the Google Cloud and writes files within the Google Drive.

The aerial descent and oceanic stability of the EDR are both premised upon having a large percentage of its total mass concentrated on one end of the shell, and this has affected our design choices appropriately. Leaving a void space at the bottom of the EDR gives us the ability to add dense material as ballast, lengthening our momentum

dipole, or the length between the geometric center of the EDR and the center of mass. A larger momentum dipole roughly translates to a more stable floating object in the ocean.

Unlike the shell, the electronic components we have used in our testing have a definitive mass, independent of the shape of the EDR. Our final electronics, detail in Section 4.2, come to 53 g. In looking at syntactic foams and potting epoxy to fill empty space in the EDR, detailed in Section 3.3, the density of these materials is another major factor we have had to research. However, there remains enough available unused mass within our mission requirements if we carefully design our shell so that we can still displace ballast at the bottom of the EDR. Since the space for the ballast is likely to be quite low, we are using a high density material for to reach our target mass. At William & Mary, we have a large amount of Tungsten powder that we can mix with potting epoxy to form an adhesive ballast. More importantly, we can change the ratio of the tungsten and potting epoxy to match any given shell shape we choose.

Ultimately, we have access to a variety of materials, but the exact masses of those materials must change for the given shape that we choose to use. In our final design, explicitly described in Chapter 6, Below is Table 2.1, which is our mass budget for our final product.

The EDR is built to withstand the impact force of hitting the ocean's surface at terminal velocity, but only from a single direction. That is, it is built to fall face-down and cannot survive the impact if the blunter, flatter base of the EDR is what strikes the water. Therefore, it must quickly self-orient in the air after being ejected from the HIAD payload. The very uneven mass distribution provided by the tungsten mass will result in just this effect. Additionally, the EDR must remain stable as it floats in the water for 30 days awaiting rescue. Although the entire device is constructed

Material	Density in kg/m3	Mass in g
Shell	1190	174.9
electronics	1366	53
epoxy	1830	30.4
foam	406	96.8
ballast	3011	75.1
EDR	924.3	430.1

Table 2.1: Multiple components comprise the EDR, each of various density and mass. Our total density is at 90% that of oceanic seawater, which gives us an upper bound on how much mass we can use given a particular shape. These masses correspond to the final product, detailed in Chapter 6.

to be waterproof, it is least likely to be damaged or lost if it can self-right to a stable floating position. By maximizing our momentum dipole, we will force that portion of the shell to always be the deepest in the water, thus keeping the shell overall upright.

Chapter 3

Non-Electronic Hardware

3.1 Shell Designs

All of the shell shapes were designed using a web-browser based AutoCAD software called Onshape. This software allowed collaboration between the five members, giving everyone access to each shell shape with the ability to make changes and additions to the design. The shapes were designed with certain requirements and expectations in mind.

- The shapes could not exceed a volume of 4 in x 4 in x 4 in. This constraint was put in place because of the size of the ejection device that will separate the EDR from the main payload.
- The mass of the EDR could not exceed 2 lbm. This constraint was put in place simply because of the total mass constraints of the entire payload. The distribution of this mass also had to be distributed in such a way that the EDR would be upright when it is floating in the water.
- The shell shapes would need to be designed in such a way that they could be perfectly sealed, as the EDR will have to withstand being in low-Earth orbit for approximately 8 hours, as well as being exposed to temperatures from -20°C to 50°C.

- One of the most important requirements that would have to be met were the forces that the EDR would experience. The shell shapes would have to be designed to withstand an ejection force of 1,525 lbf when it separates from the main payload, as well as the force it will experience when it hits the water at terminal velocity after falling from 50,000 feet.

- There were two other main requirements pertaining to seaworthiness and ability to be found, but they did not pertain as much to the design of the shell shape, as much as they did to the materials used to make the shell, and the high visibility devices placed on the EDR.

3.1.1 First Semester Shell Shapes

Cube

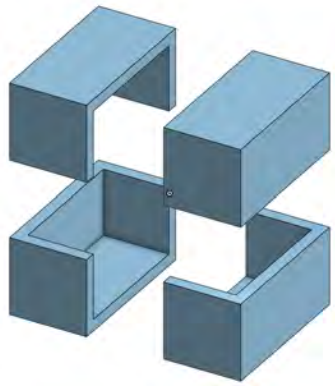

Figure 3.1: CAD design of the Cube shell shape.

The cube shell shape was a design that was made not for testing, but to create a visual of the maximum amount of space that could be used to house the components that will go inside the EDR. If the components couldn't fit in a more aerodynamic design, then the cube shape was a simple fall-back we could have. Thankfully after making 3-D representations of the components and testing to see if they fit in the more complex shapes, all of them had enough space.

Doorknob

Figure 3.2: CAD design and 3-D print of the Doorknob shell shape.

The primary inspiration of the doorknob shell shape was the basic design of a buoy[1], with the bulk of the mass distributed toward the leading end of the shape. By putting the majority of the mass in the leading (or bottom) end of the shape, it would allow the shape to fall without tumbling, allowing for the shell to penetrate the water with the curved surface, allowing for less force on impact. Having this mass focused in the bottom would also allow the shell to stay upright while remaining buoyant in the water. This will allow the solar panels we will later incorporate into the overall design to remain facing upward toward the sun, as well as keeping the high visibility device we also later incorporate on top where it will be visible.

Snowglobe

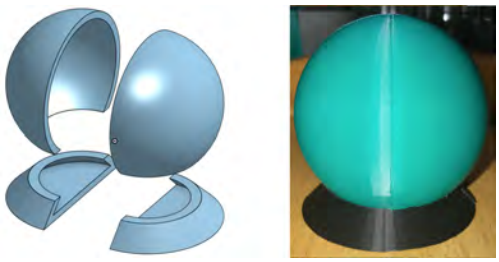

Figure 3.3: CAD design and 3-D print of the Snowglobe shell shape.

The snowglobe design, much like the doorknob design, was based off of a buoy shape, although this one is much more unique [1]. This design has two key advantages. Since the bottom surface is flat, if this is the leading end during descent, it has a very

high drag coefficient [2], decreasing the terminal velocity on descent, and decreasing the force when the shell makes impact with the water. The other advantage is that by putting the majority of the mass below the separation between the two parts of the shape, its center of buoyancy becomes very low, keeping a very large portion of the shell above the water. This allows more room for solar panels and more space to place high visibility measures, making the EDR easier to see and retrieve.

Dreidel

Figure 3.4: CAD design and 3-D print of the Dreidel shell shape.

The dreidel design is a modification of a previous design that was an attempt to model a shell shape after a NASA design found during the initial research done on possible shell shapes. This design has a cone on its leading edge that allows for easier penetration with the water resulting in reduced force on impact. The diameter of the shell shape gradually reduces from bottom to top creating more space at the bottom for the placement of components and mass. As with previous design, by keeping the distribution of the mass at the bottom leading end of the shape, it will keep the shell from tumbling on descent.

Pill

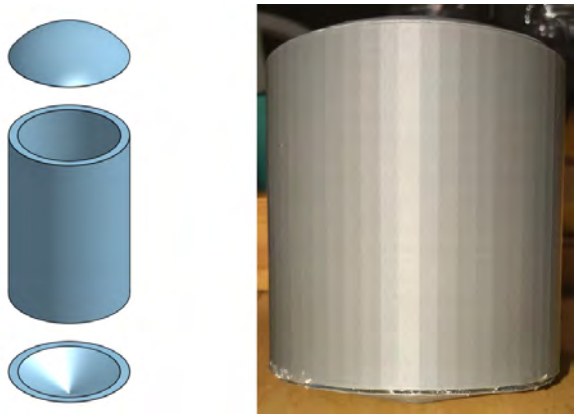

Figure 3.5: CAD design and 3-D print of the Pill shell shape.

Through analysis we found that making the shell shape longer than it is wide, reduced the force of impact with the water. The pill design was the application of that research on shell design. This design also has a lot of space inside for components compared to other designs, as it takes advantage of a lot more of the usable space along one of its axes. This will allow for possibly more inner padding and sealing inside the shell for increased protection of the inner components. As with some previous design, the pill shape has a cone on its leading edge which will also help to reduce impact force with water.

Shell Shape Testing

AERODYNAMIC DROP TEST	PILL BOTTLE	DREIDEL	SNOWGLOBE	DOORKNOB
5 feet				
0 degrees	Yes	Yes	Yes	Yes
90 degrees	No	No	No	No
180 degrees	No	No	No	No
10 feet				
0 degrees	Yes	Yes	Yes	Yes
90 degrees	No	Yes	No	Yes
180 degrees	No	Yes	No	No
20 feet				
0 degrees	Yes	Yes	Yes	Yes
90 degrees	No	Yes	No	Yes
180 degrees	No	Yes	No	Yes
COMPONENT FIT	Yes	Yes	Yes	Yes
FLOAT OVER TIME (10 min)	Yes	Yes	No	No

Figure 3.6: Summary of the data compiled through drop tests on the various shell shapes.

The first of the three tests performed was an aerodynamic drop test. Keeping the shell from tumbling on descent is a major priority, and this test was performed to compare the various shell shapes ability to achieve this. The test was preformed by first taking a 1 lb weight and securing it in the bottom of each shell. The shell was then dropped from three separate heights, with three separate initial angles at each height. Each shell would be dropped from each height at each angle 10 times. A "Yes" in the data table represents that the shell shape corrected itself during descent, and landed in the proper position, or "Stable 1" position, at least 70% of the time. The Dreidel shell shape performed the best during this testing achieving the "Stable 1" position at every variation of the test other than at 90° and 180 ° from 5 feet.

A component fit test was performed to ensure that all the shapes had enough room for the components that would later be placed inside them. Using the 3-D representations we made of the components it was found that all shell shapes had enough room for the components.

One last test was done, as a means to see if hot glue could be used as a easy sealant for tests that required no water to get inside the shell shape. This test was performed by placing the shell shapes, whose pieces were connected with hot glue, in water for ten minutes, and seeing if the shells remained floating. One problem that was found early on was that it was difficult to 3-D print the various shell shapes at there full size and in one piece, because of how long it took for printing to complete. The solution to this was to print the shapes in split apart pieces, and then connect them afterwards. An easy way to do this was with hot glue, but unfortunately it was found through this test, that hot glue is not a sufficient sealant, and can only be used on tests where the shells do not have to be water-tight.

3.1.2 Second Semester Shell Shapes

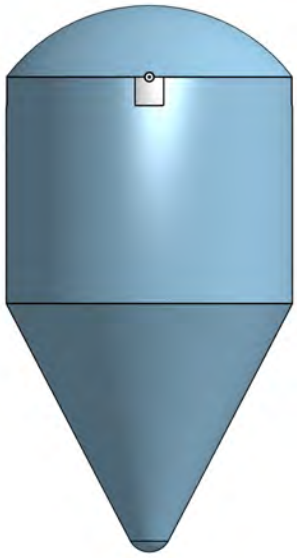

Figure 3.7: The revised pill shell shape that takes advantage of a longer cone shaped descent face to lower the force experienced on impact with the water.

This shape takes advantage of a longer cone-shaped descent face. By having this face, the force is more easily distributed and absorbed when it impacts the water. Since

the cone is more of a point and less of a flat surface, it also more easily pierces the water and negates some of the added force that the shell shape would experience from the surface tension of the water.

The main disadvantage of this shape is its relatively small size along the axis perpendicular to the direction of descent. To have such a steep cone-face and still stay within the four inch square volume requirement, the horizontal width of the pill shape could only be roughly two inches. This gives us less room to fit the required electronics inside the shell shape, as well as less room for the potting to protect the electronics.

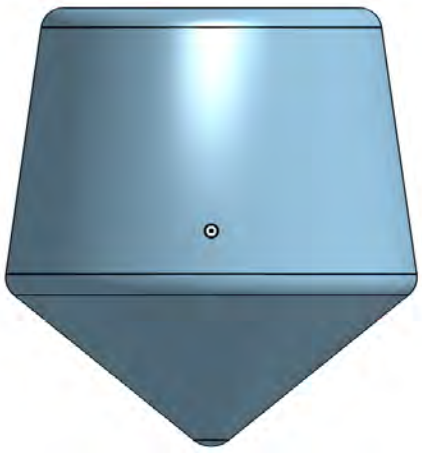

Figure 3.8: The revised dreidel shell shape that takes advantage of a large inner volume and has a shallow cone-shaped descent face.

This shape takes advantage of as much of the given four inch square volume while still having an aerodynamic shape. By doing this it unfortunately made the descent face a much shallower cone. While this increases the coefficient of drag and could possibly reduce the speed on descent, it increases the force felt by the shell shape when it impacts the water. Since the cone is shallower it also does a worse job than the pill at piercing the water and decreasing the force that the shell shape experiences because of the surface tension of the water.

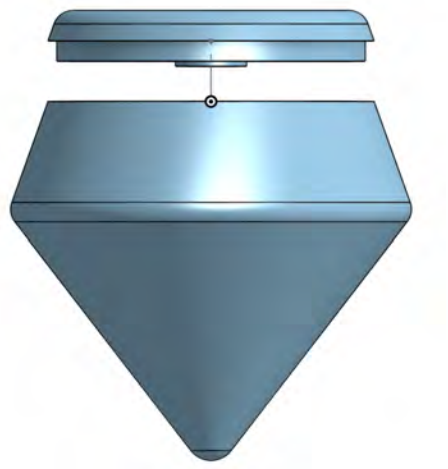

Figure 3.9: The combined pill-dreidel shell shape that take advantage of both a steep cone-shaped descent face of the pill shape and the large inner volume of the dreidel shape.

This combined shell shape takes the advantages of both the pill and dreidel shapes while also diminishing the disadvantages of both shapes.

By combining the two shapes we were able to still have a fairly steep cone-shaped descent face of 37.5 degrees. This will allow the shell to effectively pierce the water and reduce the force of impact experienced because of surface tension, as well as disperse and absorb the force experienced by impact with the water.

This shell shape also has a fairly large inner volume, especially compared to the pill shape. This will allow for us to have more freedom in how the electronics are configured inside the shell, give us more room to pot the electronics with the syntactic foam, and give us more room to place a high density mass in the bottom of the descent face to keep the payload from tumbling on descent, and keep it upright in the water.

3.2 Outer Shell Material

The initial product requirements and the nature of the EDR flight plan impose certain requirements on the material used to print the CAD modeled outer shell. The

Material	Density [g/cc]	Tensile Strength [MPa]
Windform GT	1.19	58.21
Windform SP	1.106	78.1
Windform XT 2.0	1.097	83.84
Windform LX 3.0	1.324	60.42
PLA	-	49.5
ABS	-	39

Table 3.1: A comparative reference table between the possible shell materials. Density is included because of the maximum weight requirement set by NASA LaRC, and tensile strength is included in consideration of the EDR's need for impact survivability. Specifications found in datasheets from CRP USA [4] and Farnell [5].

shell must be 3D printed using a low-cost, low-density, strong, and ocean-survivable thermoplastic. The shell must ultimately survive the force of impact upon ejection from the HIAD, impact into water at terminal velocity, and must not degrade under oceanic environmental conditions over a period of at most 30 days. As an example, Titanium might have been an ideal material, save for its high density. It is strong and ductile, has been used in aerospace applications before, and is naturally resistant to saltwater corrosion. However, the density of Titanium would be less compatible with the dipole in mass distribution we wish to achieve. Machining costs from Titanium are much more expensive than those for custom prints of thermoplastics. Additionally, since we have access to plastics via William Mary's Makerspaces, we have a deeper intuition for their strengths and weaknesses and can rapidly produce new iterations and models to test, as opposed to making assumptions about how a metal shell will act.

At the suggestion of Carrie Rhoades in the earliest weeks of the project, we have investigated Windform, a line of thermoplastics from CRP Technology, USA. The line includes several variants with differing material properties. Rhoades has seen past aerospace applications of three variants: Windform XT 2.0, Windform SP, and

Figure 3.10: Samples of PLA and each variant of Windform to be put through ocean environmental stress tests at VIMS. Samples of ABS, not shown, were taken from fragmented prints of past shell designs.

Windform LX 3.0 at NASA LaRC. We have additionally been in contact with Stewart Davis, Director of Operations at CRP-USA. Davis suggested that we focus our consideration on Windform SP, as well as Windform GT, as the two proven waterproof variants. Windform SP is conductive [7], whereas Windform GT is not [6]. Windform GT, advertised for its flexibility and impact strength, is superior to the other variants in preserving internal components upon impact [6].

Windform GT, SP, XT 2.0 and LX 3.0 are therefore the four variants of Windform which we chose to consider for the outer shell of the EDR. All four have passed outgassing tests by NASA [8], which approves them for the orbital portion of the EDR flight. However, studies have not previously been done on any variant of Windform regarding its behavior in high-saline or oceanic environments. In cooperation with the Virginia Institute of Marine Science (VIMS), we have conducted our own oceanic environmental stress tests on several thermoplastic samples (Figure 3.1), to be discussed further in section 5.1.

Five sample squares of each of the four variants of Windform were provided to us by Stewart Davis at CRP. We also included samples of PLA and ABS in the experiment, as a lower-cost material comparison.

3.3 Syntactic Foams and Potting

After considering the shell shape and material of the EDR, we are left with the internal components. While the electronics are the most important aspect of what goes inside of the EDR, we still consider all materials used for our product. If we only add the microelectronics then we have considerable void space in which those precious boards and chips can rattle around in. Thus, it is necessary to choose a void filler. While a castable foam or epoxy may seem to be an easy solution, our mission constraints, as always, influence our decision. We want to minimize the mass (at least below the 0.9072 kg mark) of our design and remain stable in the vacuum of space. Castable foams notoriously have pockets of air that will expand in orbit, and while epoxies are easier to remove bubbles from, they often are rather high in density. Thus, we looked into more specialized kinds of filler.

Upon review, we chose to use syntactic foam as our primary void filler. Syntactic foam is a combination of glass beads set within a two part epoxy, and is frequently used in the aerospace market as a lightweight option for scenarios that involve the vacuum of space. This material also comes at the suggestion of Carrie Rhoades. The EDR team has reached out to Engineered Syntactic Systems (ESS) for a test supply of syntactic foam and received pre-cast blocks. While ESS has both pre-cast and castable variants, their pre-cast product is roughly half as dense as their castable units. Thus, for the EDR bid we recommend using syntactic foam, and our version of the final product will include pre-cast cuts from what ESS has provided us.

Another consideration of internal materials in the EDR design is potting. When a suite of electronics have been assembled, it is common practice to surround the package in plastics to fill voids and bind the unit together. This reinforced package gains the properties of being more resistant to shock forces and waterproofing the

assembly. This protective layer adds to the survivability of the EDR while adding only a small amount of mass. Potting materials on Earth are typically silicon gel, thermosetting plastics, or epoxy. By the end of the semester we will choose what specific potting material to use, though for the above mentioned constraints we lean toward the epoxy option despite it having a higher density compared to other options.

Chapter 4

Electronics & Code

4.1 Experimental Configurations

4.1.1 Sandbox Drop Test

In January 2019, we determined that the shell models we were considering at the time might best be tested against each other using their defining feature: the bottom half, instrumental to both the EDR's coefficient of drag and its impact in the ocean at terminal velocity. Four shells were under consideration at the time: the Dreidel, the Pill, the Smooth Doorknob, and the Sharp Doorknob (Figure 4.1).

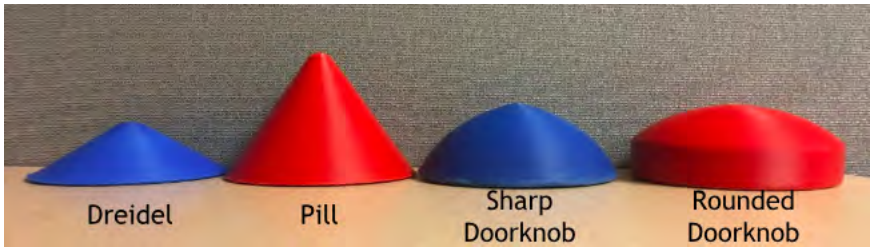

Figure 4.1: The bottom halves of the four shells under consideration at the time of the Sandbox Drop Test. Each printed at 4 in in the greatest diameter.

We designed a test that would examine the shells' deceleration upon impact in a fluid, or quasi-fluid medium, using an accelerometer-microprocessor configuration. We elected to use sand instead of water as the medium for impact, to avoid the need

of a perfectly sealed shell print. Working out a sealed design would have taken too much time in the timescale of a Sprint, and the potential for error would have put the electronics at risk, endangering the money spent on them as well. Sand was the best alternative quasi-fluid medium, which would pose far less danger to the electronic components.

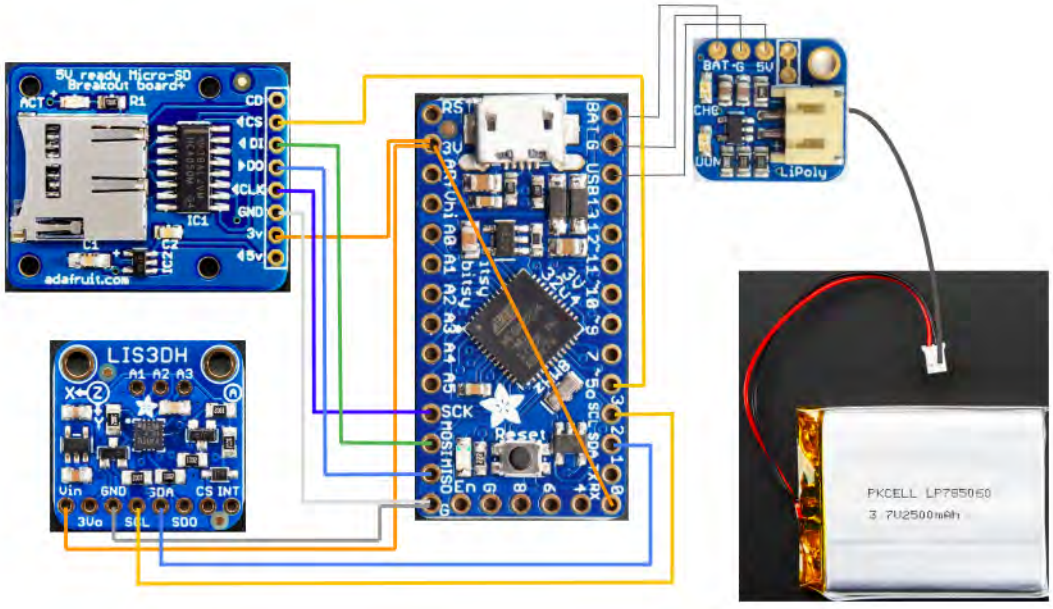

Figure 4.2: Circuit diagram of the final Sandbox Drop Test configuration, comprised of an ItsyBitsy 32u4 3V microprocessor, an LIS3DH 16G accelerometer (I^2C), a microSD extension board (SPI), and a 3.7V battery run through a regulating backpack. The relevant code can be found in Appendix A.1. Component images adapted from their respective Adafruit product pages.

There were two iterations of the test, where the second was an improvement after the errors of the first. In the first iteration, we used an Adafruit ItsyBitsy 32u4 3V microprocessor to control an LIS3DH 8G accelerometer through I^2C communication and Arduino code. There was no battery available in the first run of this test, so we had to keep the configuration plugged into a computer through a micro-USB cable. The weight of the cable, tethered to the lightweight, half-size shell bottoms we had

printed for the test altered the shells' impact in the sand. We also realized that we would need an accelerometer rated higher than 8G to register the acceleration at impact.

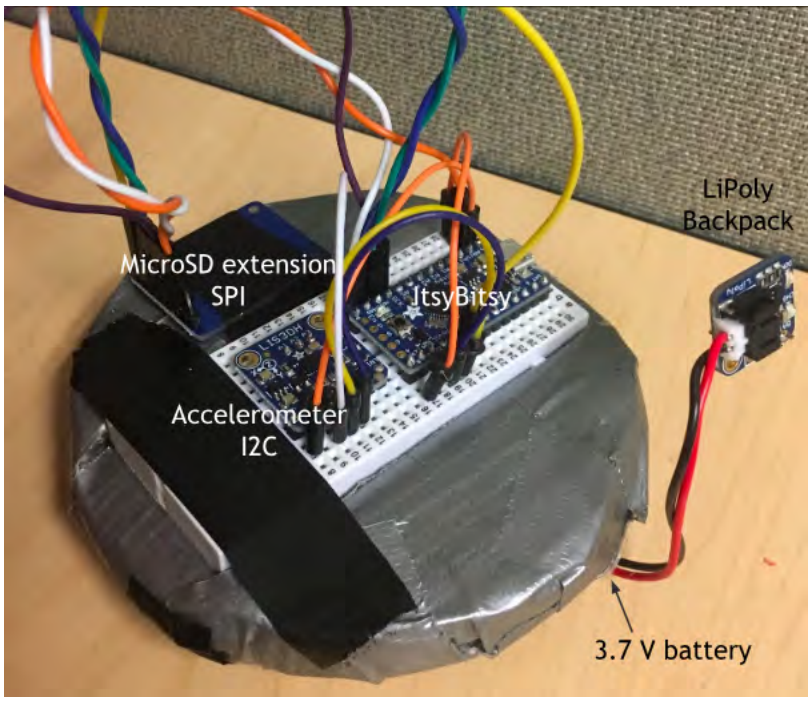

Figure 4.3: The electronics package for the final wireless version of the Sandbox Drop Test. This 4in disk was secured on each shell print under consideration. The battery is taped to center of the underside of the disk.

It is with these considerations that we redesigned the test and the electronic components to yield better data. We kept the ItsyBitsy, upgraded to an LIS3DH 16G accelerometer, and added to our circuit a 3.7V battery and a microSD card extension board, for wireless operation (Figure 4.2). The Arduino code for this configuration is detailed in Appendix A.1, in which the ItsyBitsy writes acceleration and timestamp data to the microSD card in the form of a CSV file.

We also enlarged the shell bottom prints to a 4in diameter, so that the entire circuit could be mounted on the shell during a drop (Figure 4.3). These improvements from

the first iteration of the Sandbox drop test yielded much more reliable data, discussed in Section 5.2.

4.1.2 GPS/Comms

As we approach the end of this project, we turn our attention from developing and conducting tests of the EDR shell design to formulating an electronics package indicative of the final product. The primary requirements for the EDR are to be capable of writing data to physical memory and to signal its location to our product owner. While the former task is handled through providing a component such as an SD card writer, the latter is quite a bit more involved. Additionally, as we look to the end of the year and simulating the full functionality of the EDR in a launch and recover test, developing a way to communicate location becomes vital. As such we have started a combined GPS/Coms package to address the communication of location.

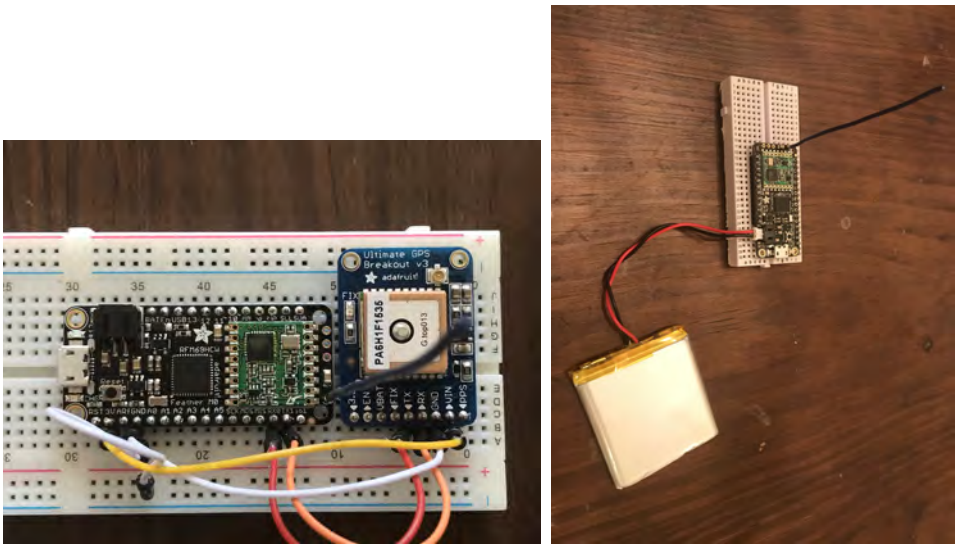

Figure 4.4: These are the electronics used to attempt location tracking and data transmission. At left, an Adafruit Ultimate GPS wired to an Adafruit Feather M0. At right, a second Feather M0 board powered by the LiPoly battery.

The GPS/Coms package is comprised of an Adafruit Ultimate GPS wired to an

Adafruit Feather M0 with an RFM69HCW chip and a second Adafruit Feather M0 with encompassed RFM69 chip. In this configuration, the Feather M0 board processes for both the GPS and an fm radio, fixing location of the combined electronics and transceiving to the second radio. While this setup is slightly more simplistic than our final goal for the bid, it suites our coding and monetary capacities.

To ensure that we can transceive and receive the location of our electronics package, we performed gradual tests of our code to ensure we can achieve our goal. For example, first we parsed location with our GPS and verified this in the serial monitor in the Integrated Development Environment (IDE). Next, we set one Feather and radio to send a message while setting the other to receive. Finally, we looped the parsed location data into the message of the sending radio and verified that our receiving radio could detect the location of the sending package.

Upon the success of the GPS/Comms test and code, we confidently move into creating a final electronics package recommendation for the EDR. The next use for the GPS/Comms code and materials is to perform a proof of concept test in which we launch a full scale EDR with GPS and Radio/Feather setup to communicate position back to a receiving Feather.

4.2 Final Product Electronics

Much of our previous electronics packaging will become vital for the final product. Alongside the above described Feather M0 microprocessor, RFM69HCW radio, Adafruit Ultimate GPS, and LiPoly battery, we will include an SDXC writer, solar panels, and are open to upgrades of components. The new items are specific to criteria for the EDR that are not present in our trials of our electronic package nor our testing of the EDR shell. To answer our requirement of writing flight data to physical memory, we plan to use an SDXC writer. This component has no need to be wired

to or otherwise utilized by our electronics package, and thus is just a consideration we must keep in mind for volume constraints. The SDXC writer will operate solely during the entry of the HIAD, and once the EDR is ejected the component ceases to run. The solar panels would answer the requirement to remain autonomous and self-powered. While recharging is crucial to the EDR as a long term component, we have received clearance from our product owner to abandon this part of the design due to the time constraints of our senior year.

At this point in the semester, we do have an electronics package for our upcoming proof of concept launch. Electronics that we are accustomed to from previous tests across the semester comprise the operating package for learning about a realistic launch scenario. We use a Feather M0 and the Adafruit Ultimate GPS to parse and relay location, while also running a 3-axis accelerometer hooked up to a microSD writer to derive information of the stability of the EDR. The package is powered by a 3.7 volt, 2500 mAhr LiPoly battery that is of similar build but smaller dimensions as compared to the battery used in the GPS/Comms test. The spatial configuration of the final package is depicted in Figure 4.5, while the wiring of the package is shown in Figure 4.6.

For the final product, it is prudent to look into the additions described above, but for our current design process they hold no useful information or immediate requirements. In terms of upgrading electronics, on a larger budget, a more consistent antenna than what comes with the Adafruit Ultimate GPS would be useful, we could swap our RFM69HCW radios for LoRa radios, and we will communicate via the iridium constellation of satellites instead of just short distance radio. While we would prefer to reach these final electronics before the end of the semester, we recognize that we had to focus our efforts toward the most mission critical aspects of the EDR first, such as floating, maintaining z-axis stability, surviving force of impact, etc.

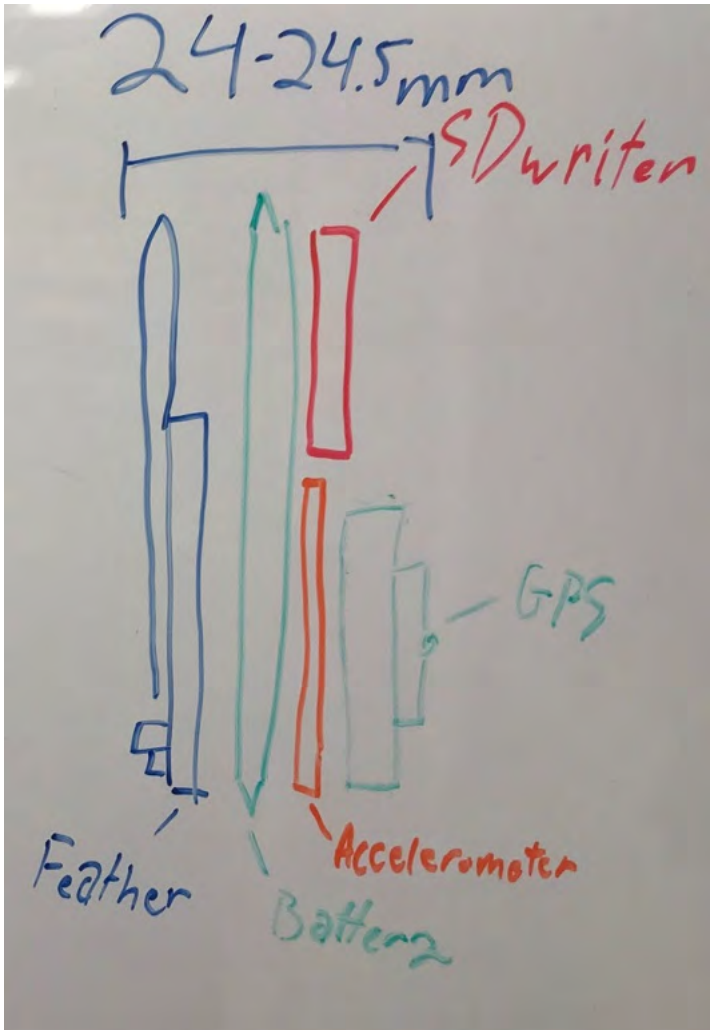

Figure 4.5: The final electronics package of the semester is made of electronics we have used previously this semester. From left to right, the Feather M0 lays against the smaller LiPoly battery, then bordered by the 3-axis accelerometer and microSD writer, finally ending with the Adafruit Ultimate GPS. This configuration centers the LiPoly battery in the middle of the electronics, minimizing the effect of non-uniform mass distribution in the EDR

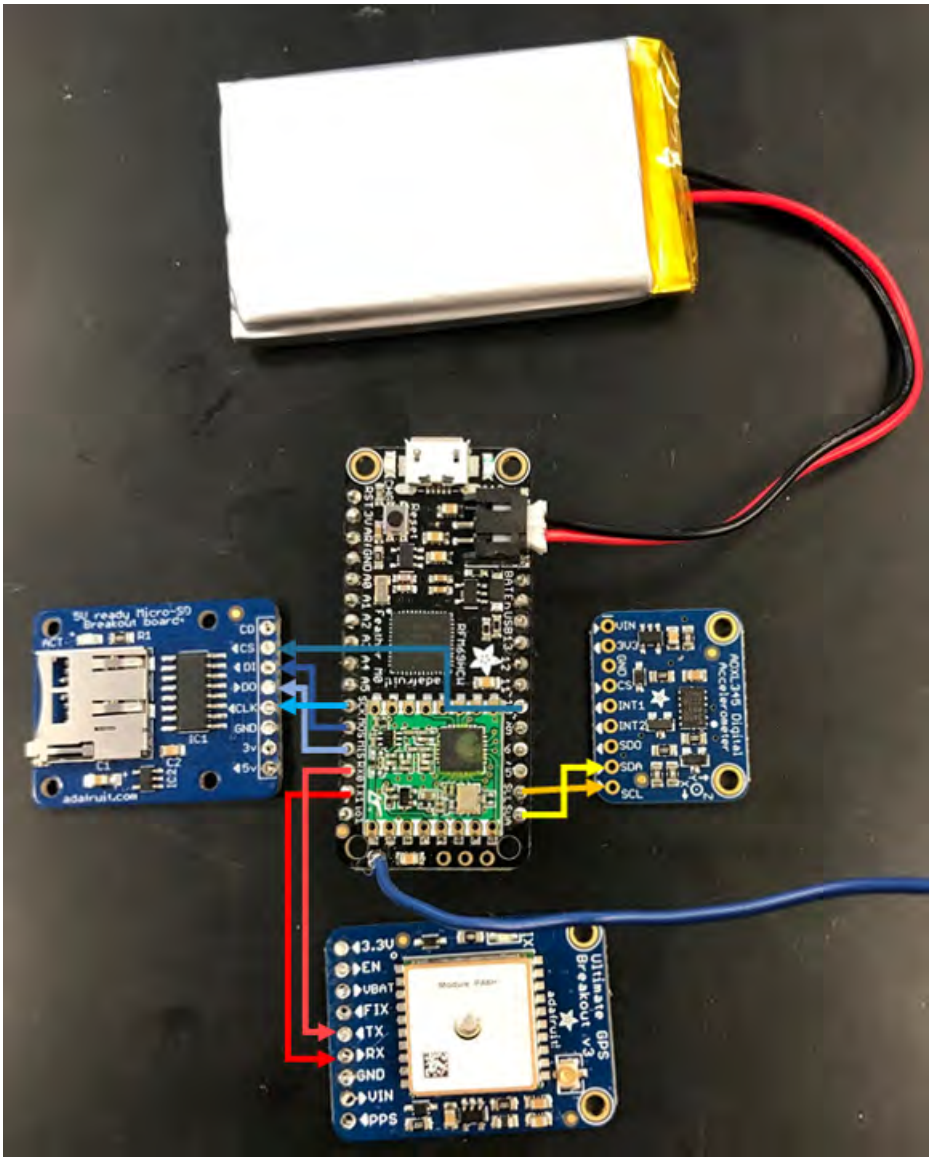

Figure 4.6: The Feather M0 is the microprocessor for our configuration, and thus is directing code for multiple auxiliary components. The Adafruit Ultimate GPS fixes a location from the satellites that it can downlink from, then sends that parsed data for location to the Feather M0, which transmits that through its radio antenna. Meanwhile, the 3-axis accelerometer parses information about the orientation of the package, which is fed back to the Feather M0 and then channeled to the microSD writer. We can run all of these chips because they are utilizing different kinds of pins from the Feather M0, be it digital or analog logic, SPL logic, or hard wiring to the transceiver/receiver pins.

Chapter 5

Experimental Methods & Results

5.1 Outer Shell Materials Testing at VIMS

To ensure ocean survivability of the material chosen to construct the outer shell of the EDR, we have conducted environmental stress tests on six thermoplastics in collaboration with VIMS, starting in late November 2018. This experiment was made possible through our connection with Donglai Gong, PhD., assistant professor of oceanography at VIMS, and Jeanna Hudson, lab and research specialist at VIMS. Gong and Hudson facilitated our access to an outdoor tank at the Seawater Research Laboratory (SRL).

The SRL tank was filled with water from the Chesapeake Bay, with added salt to achieve oceanic salinity of 37 parts per thousand [9]. We set several samples of each material in the tank for two months (double the product requirement for time in ocean), and set aside one control sample of each material. The samples set in the tank were free to float or sink, and included four samples of each variant of Windform, three samples of PLA, and three samples of ABS.

The experiment went on from mid-November 2018 to mid-January 2019. Members of the EDR team visited VIMS periodically, first every two weeks, then less frequently as we noticed little to no change in material properties. Upon each visit, we checked

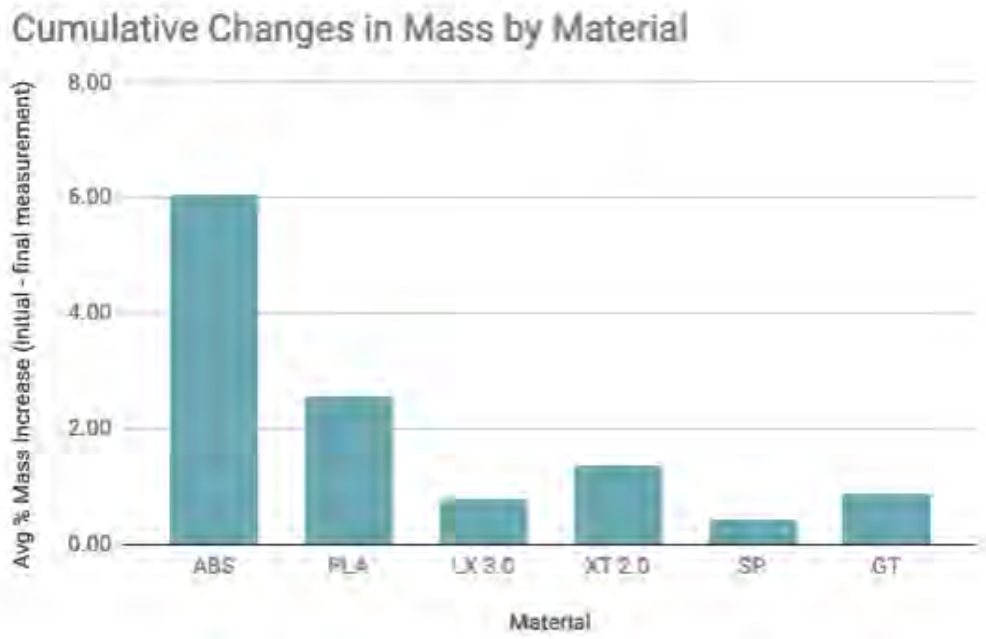

Figure 5.1: Final percent mass increases in each material (ABS, PLA, and four variants of Windform), averaged across all samples. The greater changes reflected in ABS and PLA are likely because of the lower filament density in our own prints, compared to the Winform samples given by CRP Technologies.

the salinity of the tank using a YSI meter, and evaluated the samples. We recorded the mass of each sample, and photographed one sample of each material under a microscope at 10x magnification.

We recorded the sample masses as a crude flag for the materials either taking on water and debris, or losing mass through degradation. Of course, it would be impossible to identify if both processes were present in a given sample at the same time. For this reason, we borrowed a microscope from Dr. William Cooke in the W&M Physics Department. Using the microscope, we could recognize significant changes in the material over time, and if necessary, identify the cause of such changes. We specifically looked for accumulations of salt or debris in the material, fissures, discoloration, and apparent degradation.

At 10x magnification, we attempted to photograph the materials using a microscope camera extension. However, the thickness of the samples evidently did not accommodate the focal length of the camera. The alternative was to use a flashlight for top lighting, and a cellphone camera held against the eye lens of the microscope. Aside from the occasional glare (Figure 5.2), the cell phone camera served as appropriate documentation of what we observed in the lab at VIMS.

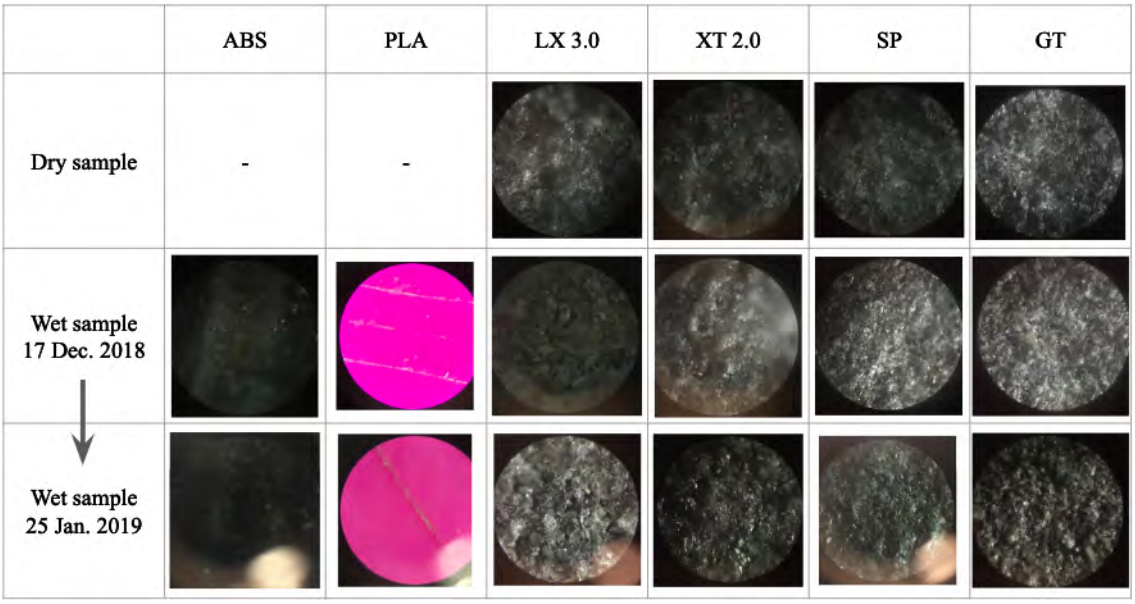

Figure 5.2: SRL test microscope images taken of each material at 10x magnification, including a dry sample, and one "wet" sample of each taken 6 weeks apart. While the wet images are of the same sample at both dates, the photos are not necessarily of the same location on each sample. All samples of PLA and ABS were set in the water before we decided to keep a dry sample of each material.

We found the greatest changes in mass in the ABS and PLA samples, and comparatively little in the Windform variants (Figure 5.1). It should be noted that the samples of ABS and PLA were printed using the default spindle settings on Flashforge and Ultimaker printers, respectively, at a much lower print density than that in the samples of Windform. The ABS and PLA samples evidently held stores of water in between the filament, which did not dry or drain before we measured the sample

masses.

Microscope images showed little material changes in the any of the Windform variants, and changes were not visibly discernible in the ABS sample. The PLA sample clearly showed salt and debris buildup in gaps and fissures in the print.

Figure 5.3: Windform GT, the material chosen to construct the outer shell of the final EDR product. It is waterproof, non-conductive, outgassing tested by NASA, and suited for cases of high impact. Image adapted from CRP Technologies [6].

Given that no variant of Windform showed any material failures which would jeopardize the EDR in the marine portion of the mission, we are free to choose the variant used in the final product according to impact and aerospace performance. The decision was ultimately between Windform SP and Windform GT, the proven waterproof variants, both previously approved in outgassing tests performed by NASA [8]. Where the two variants are dissimilar, Windform GT is non-conductive, and the superior variant in cases of high impact [6]. This is why we have elected to construct the outer shell of the EDR using Windform GT (Figure 5.3). The final print will ultimately be painted bright yellow for high visibility against the surrounding ocean.

5.2 Sandbox Drop Test

5.2.1 Experimental Setup

For the sandbox drop test we were testing the force felt by each shell shape when dropped into a fluid medium. We decided to use sand as it would not interfere and short circuit the electronics the way water would.

For both the first and second rounds of the sandbox drop test, we attached an accelerometer to each shell shape and took multiple iterations of data, dropping them from the same height for each shell shape.

Figure 5.4: The experimental setup of the first round of the sandbox test showing the 3 shell shapes we used, and the bin containing the sand with an example of the shell shape and electronics combined together for one instance of the test.

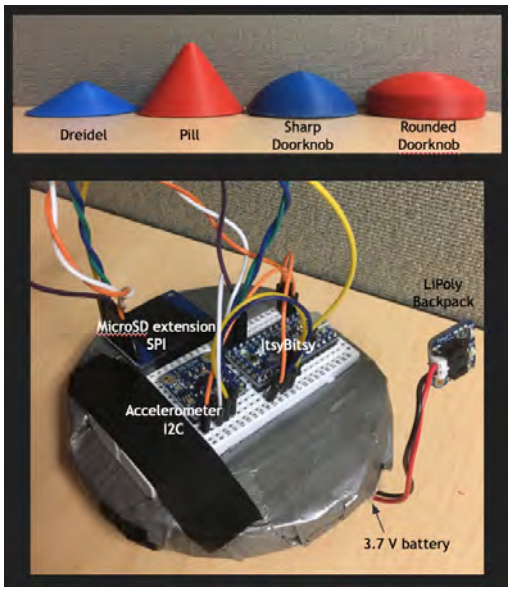

Figure 5.5: The experimental setup of the second round of the sandbox test showing the four shell shapes we used and the electronics package we made to be easily used and moved between the different shell shapes.

5.2.2 First Round of Testing

For the first round of the sandbox drop test, each of the three shell shapes were dropped three times from a height of five feet into the bin of sand.

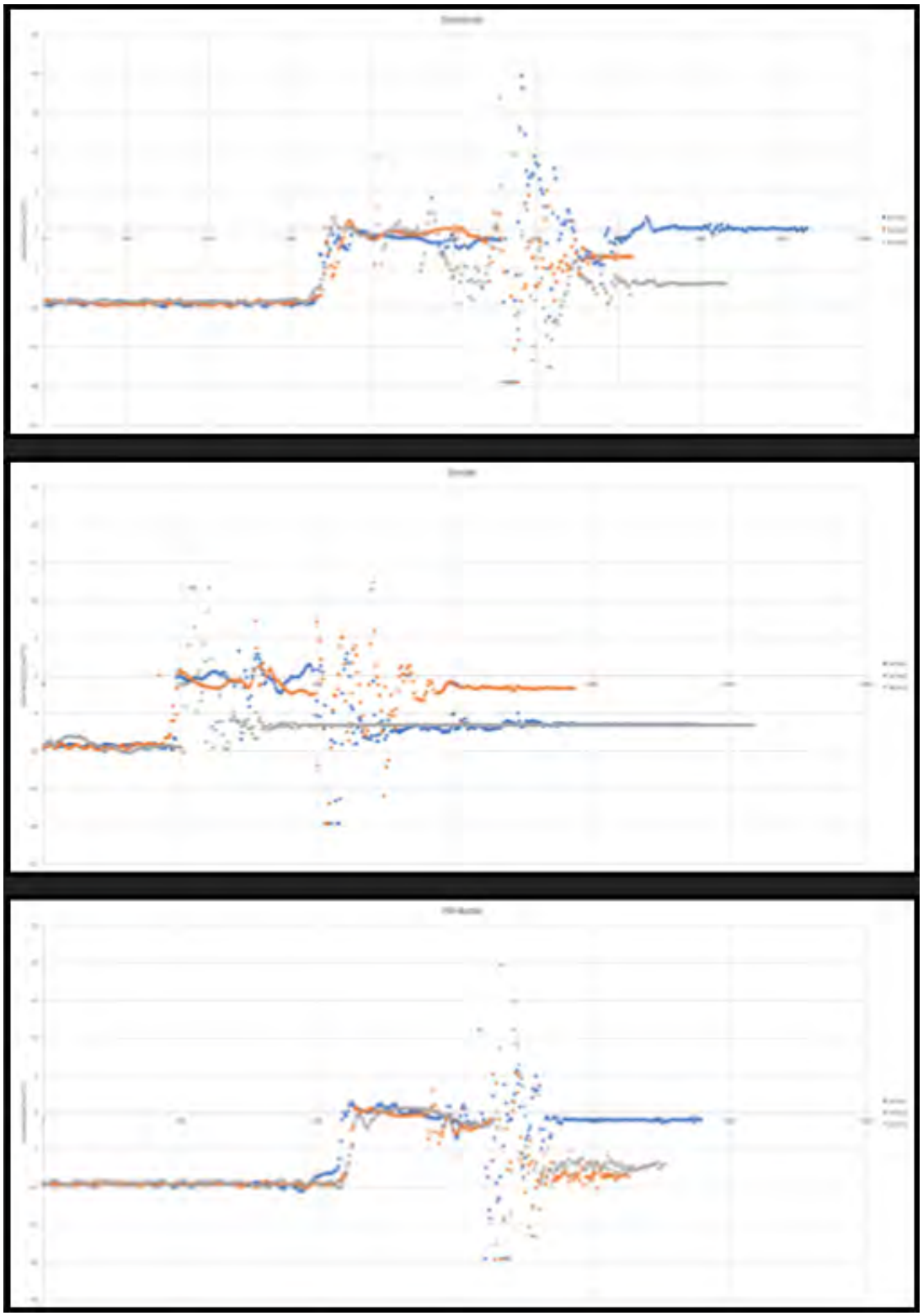

Figure 5.6: Data from the first round of the sandbox drop test showing the comparison in max acceleration for each test and each shell shape.

The first round of the sandbox drop test had multiple problems. These included the fact that we exceeded the limit on the accelerometer, and the fact that we had to have the electronics connected to the computer by a wire that effected how the shell shape dropped.

5.2.3 Second Round of Testing

For the second round of the sandbox drop test, each of the three shell shapes were dropped ten times from a height of four feet into the bin of sand. The reason for the change in iterations of the test was to increase the accuracy of the data. The reason for the change in the height of the drop was that in the first test the acceleration was exceeding the limits of the accelerometer so we changed the height to get an accurate reading from the device. We also used a SD card so that we did not have to have the electronics connected to the computer via a wire.

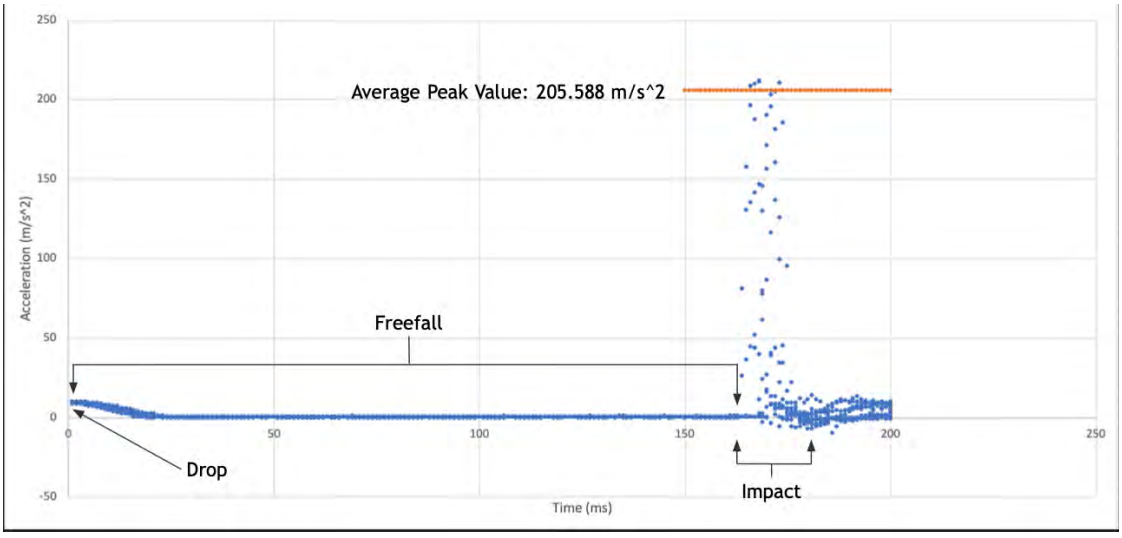

Figure 5.7: The data for the second round of the sandbox drop test, for the pill shell shape showing the average peak acceleration felt by the shell shape.

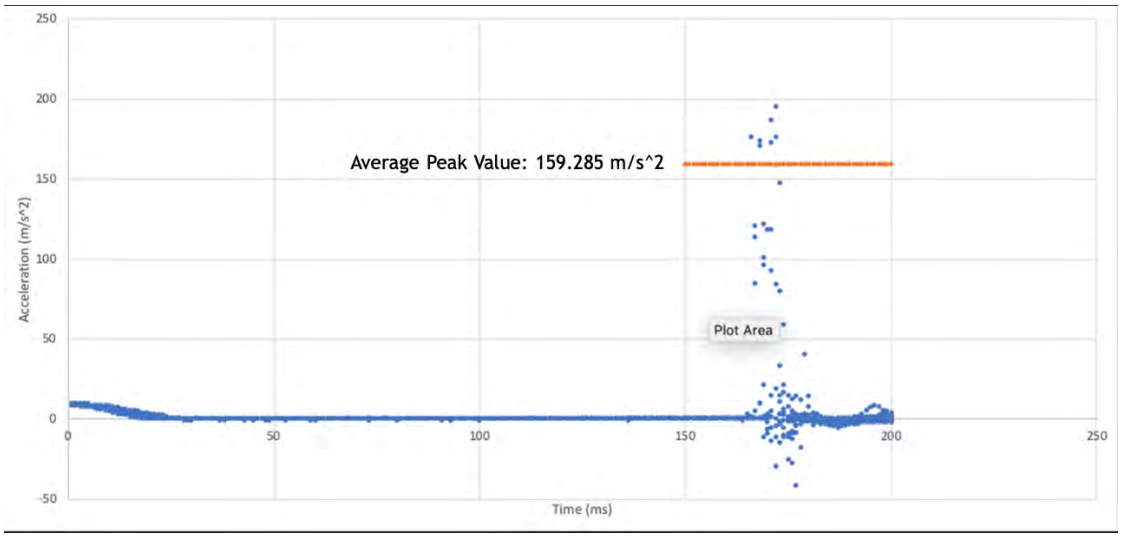

Figure 5.8: The data for the second round of the sandbox drop test, for the dreidel shell shape showing the average peak acceleration felt by the shell shape.

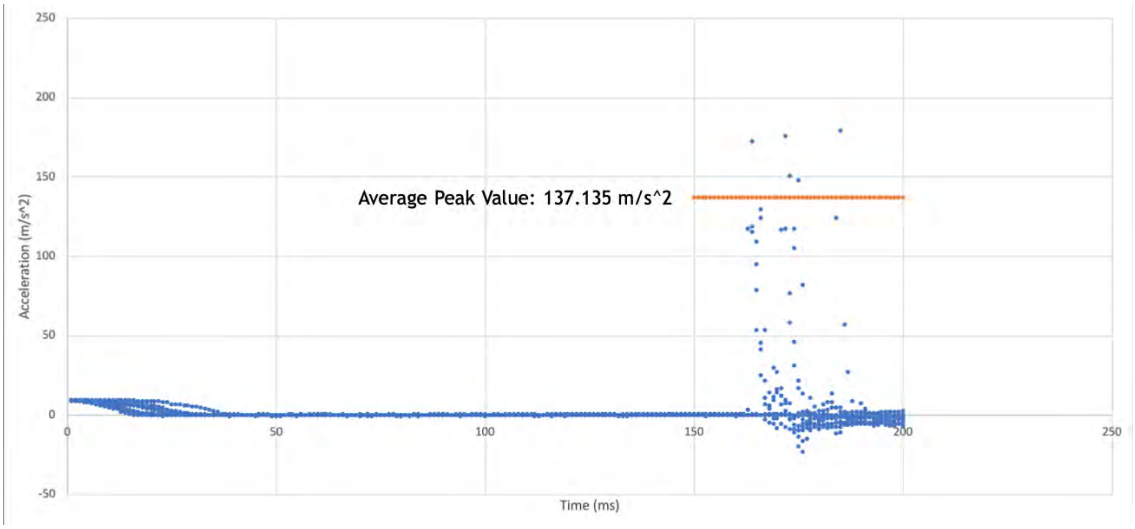

Figure 5.9: The data for the second round of the sandbox drop test, for the sharp doorknob shell shape showing the average peak acceleration felt by the shell shape.

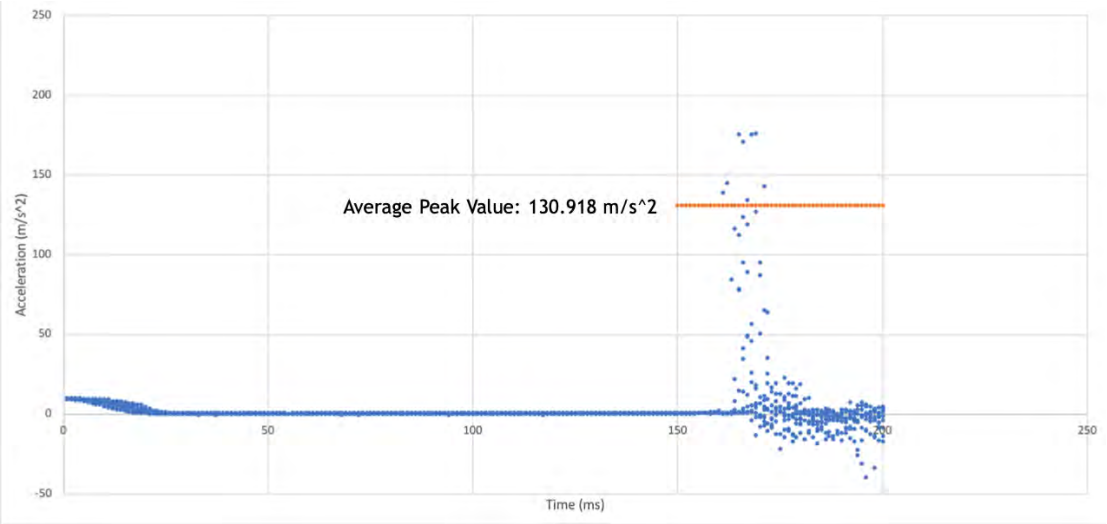

Figure 5.10: The data for the second round of the sandbox drop test, for the rounded doorknob shell shape showing the average peak acceleration felt by the shell shape.

SHELL SHAPE	ACCELERATION (m/s^2)
Pill	205.588
Dreidel	159.285
Sharp Doorknob	137.135
Rounded Doorknob	130.918

Figure 5.11: A summary of the peak acceleration experienced by each shell shape in the second round of the sandbox drop test.

In the second round of testing we were able to better see the difference in peak acceleration experienced by each shell shape. Through the testing we were able to find that the rounded doorknob had the lowest peak acceleration. While this round of testing did give us better data, it was still flawed in that the acceleration recorded for the pill shell shape was over the acceleration limit for the accelerometer. However, it still gave us a good side by side comparison of the acceleration experienced by each shell shape.

5.3 Slow Motion Lateral Launch

The goal of the lateral launch testing that was conducted was two-fold: to determine how qualitatively aerodynamic our weighted shell shapes were at high speed, and to analyze an impact with a water target.

In order to simulate the impact of the EDR in practice, it was necessary to imitate an impact that is closer to the actual speed of the fall. In order to do this without a natural vertical fall, a test was conducted that involved an artificial ejection oriented horizontally.

Such an ejection was achieved utilizing a homemade air cannon. The cannon consisted of a closed chamber into which air was pumped, an open chamber into which the object in question was placed, and a valve that controlled the air flow from the closed chamber to the open one. Built to accommodate miniature models of the shell shapes, the cannon was constructed from 2 inch diameter PVC pipes.

The design of the launch had the air cannon laying horizontally on the ground with slight elevation to assist with aiming. The controlled variables of the launch included weighting each miniature shell shape used with a 0.4 lb $\frac{3}{4}$" ball bearing at the tip, and the amount of air pumped into the closed chamber for every launch trial was kept at a constant 3 bars of pressure. Air was pumped using a standard bicycle pump.

Figure 5.12: This is the air cannon used in the lateral launch tests. Next to it is the bicycle pump used to pressurize the closed chamber for each launch.

Placed a certain distance in front of the open chamber of the cannon was a target consisting of a 1 gallon Ziploc bag filled with water. The target was propped within a foot in front of a black and white checkerboard backdrop with evenly sized 10 cm diameter squares to measure relative distance.

Figure 5.13: Here are still frames of the dreidel-pill miniature shell shape piercing the water bag target. Taken with the Edgertronic SC2+ slow-motion camera.

Video of every ejection trial was taken using an Edgertronic SC2+ slow-motion camera connected to a power source via an extension cord and a computer via an Ethernet cable. Initial trials utilized a frame rate of 4000 fps in order to analyze the projectile motion of the shell shape, but that did not end up being sufficient for some quantitative analyses, so later trials took advantage of an increased 7000 fps.

Shell	Test #	Pre-impact					In bag					Post-bag				
		Distance [cm]	p/m	Frames	p/m	Speed [m/s]	Distance [cm]	p/m	Frames	p/m	Speed [m/s]	Distance [cm]	p/m	Frames	p/m	Speed [m/s]
Dreidel	1	11	0.1	30	1	25.667	14	0.5	59	2	16.610					
	2	11	0.1	30	1	25.667	15	1	60	6	17.500	6	2	62	4	6.774
Pill	miss	22	0.2	48	1	32.083										
	1					#DIV/0!					#DIV/0!					#DIV/0!
	2					#DIV/0!					#DIV/0!					#DIV/0!
Dreidel-Pill	1	11.5	0.2	31	1	25.968	16	1	81	6	13.827	9.5	0.5	122	2	5.451
	2	11	0.1	31	1	24.839	18	0.5	90	4	14.000	10	0.5	73	2	9.589

Figure 5.14: The data collected in the second iteration of the lateral launch test. Shown are the derived speeds of each shell shape pre-, mid-, and post-impact. One outlier is the pill, which overshot the target and broke on impact with the back wall, causing a break in salvageable data.

Using the iteration of testing that resulted in cleaner 7000 fps video, said video was analyzed frame by frame utilizing the standardized backdrop in order to derive an estimate for the shell's flight speed and deceleration into the bag of water. Initial

launch speed estimates brought the Dreidel and Dreidel-Pill hybrid shapes to similar readings of 25 m/s within error with two trials each. Deceleration within the water was decidedly higher for the Dreidel-Pill shape, being slowed by the water an average of about 3 m/s more than the Dreidel.

In a majority of the trials, the shell shapes pierced the bag, fully exiting through the back side. These two layers of plastic certainly took a non-negligible amount of kinetic energy to pierce It should be noted that the experimental design of this test was flawed for this reason. However, while a plastic bag filled with water is not a completely accurate representation of an impact into an actual free body of water, given the limitations of our testing apparatus it was a considerably worthwhile test that aided in the choosing of the final shell shape design.

5.4 Graveyard Tests and Analyses

Throughout the whole of this developmental process, there have been several times when a test or calculation was well-intentioned but either lacked a proper execution, methodology, or was conceptually misguided. It is important to acknowledge such setbacks as a sign of continued adaptation and growth upon the receipt of new information, as not all endeavors taken as a step toward a final product have been necessarily helpful in the long run. This section will be used to outline these endeavors.

5.4.1 Force of Impact Modeling

The use of the EDR in flight tests for a HIAD device comes primarily in three stages: the ejection from the HIAD payload and descent, the moment of impact with the ocean's surface, and the subsequent oceanic recovery period of up to thirty days. The most immediate way for the EDR to fail in its mission is if it were to break at the

moment of impact, and so a large portion of our design work has been to prepare for this shock.

In order to calculate the force that would have been imparted to each shell shape, a numeric force model was created in Colaboratory, a collaborative coding interface that utilizes Python. However, there were holes in the usage of this analysis method. Firstly, several unknowns were assumed in the calculations for each shape, causing the data derived to be very general and not specifically tailored to the shapes. Secondly, the numbers that were obtained were far higher than intuition based on previously done, simpler calculations would allow, causing the model to be doubted in terms of accuracy of at least one or more of its components. Thirdly, there was much mixing between the usage of SI units and Imperial units throughout the initial computation process, which was a point of contention that the group quickly realized needed to be addressed early on.

More specifically, in the analysis of the force of impact, our assumptions vastly favored denser shapes, so decreasing the volume of a given shell design will increase our plunge depth and decrease our resulting force of impact. Our set of assumptions did not work well with shapes of low coefficient of drag, which do have high terminal velocities but dissipate force by plunging deeper than high drag shapes. As such, in deciding whether to optimize plunge to dissipate energy, the model became increasingly less accurate and reliable than anticipated.

5.4.2 Undriven Damped Oscillation Float Test

An early iteration of float testing that was done near the end of the fall of 2018 was a test on each shell shape's undriven damped oscillation in water. This test utilized a motion tracking software to track the motion of a flag extending from the top of each shell shape as it gradually corrected itself towards equilibrium.

The main flaws in this test lie in the experimental design. Firstly, the shell shapes used were not full shapes, but shapes printed in quadrant sections that were hot glued and/or duct taped together. This was not representative of a perfectly printed shell shape. Additionally, the weighting used was 85g of ball bearings, which meant that none of the weight distributions were equivalent or constant in any way, as they were able to shift without warning or control. Third, the environment of the test was not analogous to an actual turbulent environment so it didn't yield much useful data in the end.

5.4.3 Force of Impact Drop Test

The initial drop test that we conducted was one in which the force of impact was analyzed in reverse to the actual conditions. That is to say instead of dropping the shell shapes with weight, weight was dropped onto the shell shapes themselves. Trials of increased weight being dropped on the same shell shapes were conducted based on calculated Joule energy transfers that were assumed to be analogous to the terminal velocity impact calculations.

The flaws in this test lie in the assumptions made. It was unclear what the data collected would be describing, as it was simply a repeated stress test rather than an actual impact test. Repeated trials on the same previously crushed shell shapes with increased weight were not useful in showing its strength in a one time impact, as is the reality of the EDR's purpose.

Chapter 6

Conclusion/Outlook

During the weighted drop test it became apparent that the modified Dreidel shell shape design was the highest performer in terms of the shell being able to correct itself to the "Stable 1" position during descent. The Dreidel was the only shape that was able to achieve the "Stable 1" position at the 10 feet and 20 feet height for the 90° and 180°. The doorknob was the next most successful shell shape as it was able to achieve the "Stable 1" position at the same positions as the Dreidel except at 10 feet at 180°. The pill bottle and snowglobe shell shape both performed poorly, but may be able to achieve the "Stable 1" position when dropped from a higher height.

From these results in addition to the results of the lateral launch slow-motion testing it is apparent that the modified Dreidel-pill hybrid shape with a 37.5° cone is the best shell shape in terms of aerodynamics and has the potential to become our final shell shape.

Since the end of the fall semester, we conducted further quantitative tests on improved designs, and began blueprinting the interior of the EDR. The end goal of the spring semester is to hold drop tests and trial retrieval runs on functional prints of our top shell shape. Further tests on the shell have and will include more scrutinizing static float tests, dynamic float tests in turbulent conditions, and GPS/radio communications tests. We also hope to eventually test the G limits of the perspective

electronic components, possibly through parabolic launch tests via the air cannon.

These tests will include cheaper versions of all electronic components that will be used in the final HIAD flight tests. Although design of the electronics configuration was not an initial expectation from the product owners, we strove to have a fully functional EDR design, by the end of our year of research. The hope is that our final design will be tested exhaustively, such that it is entirely ready for HIAD flight testing. The final blueprint will comprehensively describe to engineers at NASA LaRC how to construct the EDR, once they are ready to begin on-Earth flight testing on the HIAD.

6.1 Final Product

At the end of our ninth and final sprint, we have produced a workable model for the EDR but are lacking several of the key elements required for a final product. A great proportion of the research performed and the experiments conducted have related to the outer shell of the EDR, and how it should be designed. In this respect, we have largely completed our work and arrived at a finalized shell construction (Figure 6.1).

The overall shape of the outer shell has been the single greatest sticking point in our designs. We initially began with a multitude of different of different shapes (including a 4" cube that would occupy the entire allowed volume) but quickly reduced this down to four "finalists": the snowglobe, doorknob, dreidel, and pill shapes. Between these four however, it was much less clear which shape is best. The broader doorknob had the greatest coefficient of drag, while the streamlined pill could pierce the ocean's surface most effectively. We were encouraged by Ms. Rhoades and Dr. Deconinck around the mid-year point to hold off on making a final selection a take options off the table early. This proved sound advice, because it was not until well into the spring semester that we finally converged on the "Dreidel-Pill" shape as

our selection. This had not been on the table previously and might not have been conceived had we forced the group into an early decision on it.

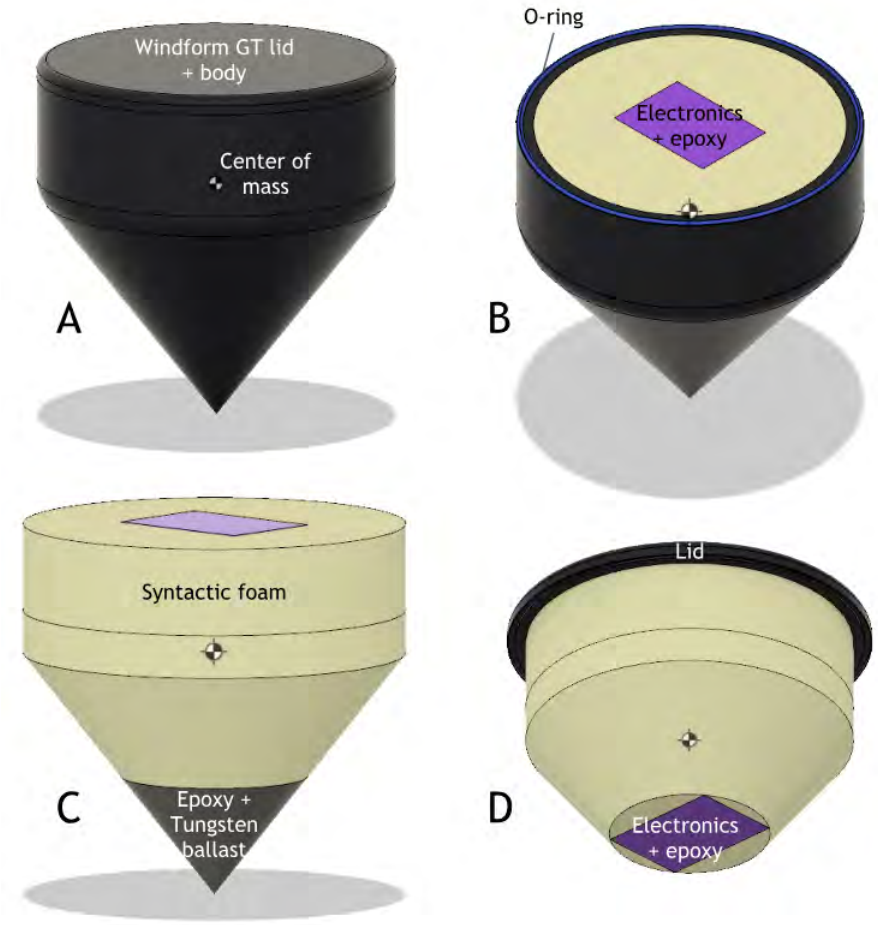

Figure 6.1: CAD model of the near-final product, done using Fusion 360. (a) The outer shell, comprised of a body and lid. (b) The shell is sealed with an o-ring at the interface, and the electronics are potted in a block of epoxy set within the syntactic foam. (c) Beneath the syntactic foam is a ballast, made of epoxy and Tungsten powder. (d) The electronics fit perfectly within the syntactic foam.

The choice of material with which to construct the EDR's outer shell was made similarly late into the process. Our two-month collaboration with VIMS to test the effects of a marine environment on varying materials did not come to an end until late January, meaning we could not make an informed decision prior to that point.

Although nearly all of the materials used (ABS, PLA, several Windform variants) demonstrated adequate survivability in the saltwater tank, Windform GT was chosen for its proven performance in impact.

The electronics that will run inside of the EDR are less of a final product. In sprints eight and nine, we finally began testing some of the software features of the EDR, including its ability to locate itself and send that information to NASA. We were able to successfully build and program a microcontroller to read its location on command and send that data as text to a distant source. Additionally, we managed to gather an arrangement of electronic components that are al compatible to be used together (in terms of current draw, voltage requirements, etc.). However, these are not the components which will be used in the final product if NASA chooses to use the EDR. The Adafruit Feather M0 will most likely be replaced by a Beagle board, the RFM69HCW packet radio could be swapped for a device that uses LoRa, and and the Adafruit Ultimate GPS we used would become an Iridium Constellation device in the final product. Although we achieved much of the functionality of the electronics required, we were not able to design or construct a model that utilized components which could serve in the actual HIAD flight test.

As it stands, the EDR is a fairly fleshed-out concept – the structure necessary to survive its mission and the functionality to perform its job have been achieved by our team. However, there are a number of features that will be addressed in section 6.2 that have not been part of our design. Future teams or persons who are interested in taking this design further should definitely incorporate these features into their work, including NASA if the EDR is used in the HIAD flight tests.

6.2 Future Steps

In order to complete the final steps in regards to a flyable product that is in practice fully utilizable by NASA's HIAD mission, there are several features of the EDR that are either required by the mission specifications or requested by NASA that we did not address in our design of the EDR. This section is where they shall be touched upon.

The first, most pressing detail is the current lake of an external sealed USB port. Being a data recorder requires the capacity for data to actually be recorded, which includes the ability to write data onto the internal SD card that will necessarily be a part of the final product. As such, an external USB must be included to allow the payload of the HIAD to write its data onto the SD card while in its pre-ejection positioning. This needs to be sealed such that the internal SD card is not damaged by the seawater on impact or during its time floating in the ocean.

Another similar design element that went unaddressed is how the EDR will be sealed and waterproofed. Several ideas, such as using an O-Ring or a mechanical seal with screw mounts have been discussed. Most promising is the concept of 3d-printing the EDR's outer shell around the electronic components being used as one solid piece, so that there is no gap to seal at all. However, none of these have been fully explored.

Another main concern to consider in the future is the communicative ability of the EDR, and as an analog, the internal power capabilities of the EDR. To maintain a strong connection with the radio/GPS components, it should be advantageous to attach some sort of extendable antenna that can deploy upon impact and aid in signalling.

To make sure the EDR remains powered throughout the duration of the search, it is necessary to have a charging method to maintain a continued power supply to

the internal components. A power source that will last for thirty days at sea is one main requirement given by NASA. We have considered the use of flexible solar panels along the exterior of the outer shell to address this issue, but have not performed significant research into the costs, benefits, or feasibility of such a solution. In the event such an addition can be made, it will ensure that a continuous source of charge will be available to the EDR's internal battery during the search and rescue.

Finally, a necessary component to the successful search and rescue of the final product is an element of high visibility. This is essential to ensure the quick and easy location of the minuscule EDR in the turbulent ocean waters in tandem with the GPS. This would involve several options, such as an outer coating of bright yellow or international-safety orange paint to contrast with the blue waters, as well as an LED beacon to place on the top of the shell to assist in visibility.

6.3 Agile Retrospection

Upon retrospection of how well the Agile Project Management Process was implemented for our project, there were three major areas that we could improve upon.

The first is in that we should have met with the people involved with the entire project. In the Agile process it is important for all teams involved in the design and development of the final product to meet, usually every 10 weeks. This allows for the transfer of all knowledge of information and problems experienced by each team so that everyone is on the same page and knows what need to be done to most efficiently get to the final product. For our project we only met with the people involved with the overall project for the first two sprint meetings. This made it very hard to communicate with them on some of the requirements of our project and made it take more time than necessary to get responses on how best to proceed with certain elements of our design.

The second is that we should have worked together in the same place much more than we did. Due to the fact that we are all seniors in college it made it very difficult for us to line up our schedules so that we could all be working in the same place at the same time. We all had different class schedules and different obligations that we had to be at throughout the day, so the only time we had that we could communicate in person with one another was at the sprint meetings 3 times a week. In the Agile process the scrum teams work together almost exclusively so that the transfer of information can be instantaneous and efficient.

The third is that we should have should have been able to spend more time working on the project. Again due to the fact that we are in college,it is impossibly for us to commit as much time to the project as people who are normally implementing the Agile process would be able to give. In the Agile process people are working on their designated project full time and don't have any other commitments that they have to give their time too. For our project we both had to commit time to the design of our product, as well as committing time to a full class schedule.

6.4 Author Contribution

William Bushman served as the team's Research Librarian. His role was to discern the necessary information for the group to know in each area they worked, and to streamline the important knowledge for others in order to avoid time being wasted learning non-relevant information. He wrote Sections 1.1 regarding the context and purpose of the EDR, 2.2 summarizing the internal mass distribution, and 6.1 reflecting on the progress made toward a viable final product, along with light editing throughout Chapters 4 and 5.3.

George Denny served at the team's Scribe. His role was to record notes from

meetings, both our thrice a week 10 minute meetings as well as our formal sprint presentations. Additionally, he made physical representations of the interior components to our EDR, printed the shells, made the model for impact force, worked collaboratively on the VIMS material tests, assissted with data taking for the slow motion impact test, and wrote a script to determine the ratio of tungsten to potting epoxy to obtain the most optimal mass distribution. He wrote Section 1.2 and 3.3 regarding the concept of operations for the HIAD and the Syntactic foam/potting epoxy, Section 4.1.2 and 4.2 regarding the GPS/Comms Electronics and the Electronics of the final package, as well as the theory and model of force of impact and the mass budget within the mass distribution.

Nathan McConnell served as the Team Leader for our research group. As the team leader his roles consist of making sure everyone stays on track and completes their respective tasks on time, as well as making sure that the meetings run smoothly and are completed on time. He wrote all of Section 1.3 on Product Requirements, Section 3.2 on shell designs, Section 5.2 on the Sandbox Drop Test, Section 6.3 on Agile Retrospection, as well as the first paragraph of the conclusion.

Aurora Santangelo served as the team Ambassador. Her responsibilities included communicating with outside parties on behalf of the team, such as VIMS, CRP Technologies, and members of the W&M community, and maintaining the team website (TeamAgileImpact.com) to publicize the project and design progress. She wrote Section 1.4 on Agile methodology, Section 3.2 on outer shell materials, Section 4.1.1 on the Sandbox drop test electronics, with code in Appendix A.1, and Section 5.1 on materials testing at VIMS.

Rollin Woodford served as the team's "Devil's Advocate." His responsibilities in-

clude analyzing different aspects of designs to establish the pros and cons of each option. He has conducted velocity analysis and preliminary float tests on our initial half sized models, as well as handled the air cannon during the first round of lateral launch testing. He wrote Sections 2.1 on the theory and analysis of terminal velocity, 5.4 on the scrapped testing and analyses, and 6.2 on future steps.

Appendix A

Library of Code

A.1 Sandbox Drop Test

The following is the Arduino code used in the final version of the Sandbox Drop Test, detailed in Sections 4.1.1 and 5.2. This code is intended for an Adafruit ItsyBitsy 32u4 microprocessor, an LIS3DH triple-axis 16G accelerometer (I^2C), and a microSD card extension board (SPI).

After setting up serial connection at a baud rate of 115200, the ItsyBitsy tests its connection with the accelerometer, and sets the sensor to a max of 16G acceleration. It then confirms connection with the microSD extension board, and opens a new text file on it. In the loop, the ItsyBitsy retrieves accelerations along the x, y, and z axes, along with a time stamp. The z-acceleration was relevant to our test, given the orientation of the electronics on the shell prints (Figure 4.3). The z-acceleration in SI units and time in milliseconds is then written to the file on the microSD in the form of a CSV file, ready for data analysis.

Because it is can be difficult to break the main loop in Arduino, but the file must be closed to be properly saved, the solution was a kill pin. Pin0 on the ItsyBitsy is always tied to 3V during a drop. If pin0 is ever read low, it will close the file, and then wait a 30 second delay. In this time, one could remove power from the whole

circuit, preventing the ItsyBitsy from attempting to start the loop once again.

```
/*********************************************************/

/*   Aurora Santangelo, adapted from Adafruit Learn Adruino guides
for ItsyBisty, LIS3DH accelerometer and microSD extension board   */

#include <Adafruit_LIS3DH.h>
#include <Adafruit_Sensor.h>
#include <SD.h>

File myFile;

Adafruit_LIS3DH lis = Adafruit_LIS3DH();
int inPin = 0;
unsigned long time;

void setup() {
  Serial.begin(115200);
  delay(1000);

  pinMode(inPin, INPUT);

  // Set up accelerometer connection
  Serial.println("Testing LIS3DH!");
  if (! lis.begin()) {
    Serial.println("Couldnt start");
    while (1);
  }
  Serial.println("LIS3DH found!");

  lis.setRange(LIS3DH_RANGE_16_G);   // 2, 4, 8 or 16 G
  Serial.print("Range = "); Serial.print(2 << lis.getRange());
  Serial.println("G");

  // Set up microSD connection
  Serial.print("Initializing SD card...");
  pinMode(7, OUTPUT);
  while (!SD.begin(7)) {
    Serial.println("initialization failed!");
    delay(1000);
  }
  Serial.println("initialization done.");

  // Open the file.
  myFile = SD.open("sharp_doorknob.txt", FILE_WRITE); // Change file name here

  // If the file opened okay, write to it:
  if (myFile) {
    Serial.print("Writing to test.txt...");
```

```
    myFile.println("********** testing 1, 2, 3 **********");
    } else {
    // If the file didn't open, print an error:
    Serial.println("error opening test.txt");
  }
}

void loop() {
  while(1){
    // Get a new sensor event, normalized
    sensors_event_t event;
    lis.getEvent(&event);
    time = millis();

    // Formatted for CSV
    myFile.print(time);
    myFile.print(",");
    myFile.println(event.acceleration.z);

    // Close file and 30s pause to unplug battery from board if pin0 low
    if (! digitalRead(inPin)){
      myFile.close();
      Serial.println("done.");
      delay(30000);
      break;
    }
  }
}
```

A.2 Mass Distribution Calculator

The following is the Python 3 code used to develop the Mass Distribution and Mass Budget of the EDR, detailed in Section 2.2. This code was developed in Colaboratory, a Python 3 Integrated Development Environment (IDE) in the Google cloud that allows for multiple individual to work on a shared document, although it should run in any IDE.

First, we import some tools from the Python Math code library. Next, we determine the density of the sample of syntactic foam we received from Mr. Thom Murray from Engineered Syntactic Systems. After that, we define the spacial constraints of the electronics package. Following that, we determine the volume of the shell, syntac-

tic foam with a hole for the electronics and potting epoxy, the volume of the potting epoxy, the volume of the electronics, and the volume of the space left for ballast at the bottom of the EDR. Then, we use the densities of the above described components, calculate the target mass for the EDR by deciding how much of it should float above the water line and using Archimedes Principle, and determine how much mass is left over to be used as ballast. Afterward check to make sure that we have enough excess mass budget to use epoxy and tungsten, and calculate the ratio of tungsten and epoxy to achieve our desired mass.

Several variables are called to print, often without their units in the print command. The units are always commented somewhere within that code cell, but only the the last several cells give outputs that an interpreter needs to use.

```
from math import pi
from math import tan
from math import log
from sympy.solvers import solve
from sympy import Symbol
import matplotlib.pyplot as plt
import numpy as np

# Finding the density of our Syntactic Foam, we need to be more precise than
# the distibutor's number

m_prism = 0.676

v_pris = 0.00166842
v_pris_2 = 0.00166403
v_pris_3 = 0.00165748

rho_p_1 = m_prism/v_pris
rho_p_2 = m_prism/v_pris_2
rho_p_3 = m_prism/v_pris_3

print("our densities for the pris foam are ", rho_p_1, ", ", rho_p_2, ", and ", rho_p_3)

# Let's figure out what's up with our electronics, meters are units
# z is long
# x is wide
# y is thick
```

```
# thick is weird because boards and chips are not uniform. Using this as a bound
# for the hole for the electronics, but multiplying by 0.7 for the volume for the
# electronics themselves as we think about the volume for the epoxy filling the
# void space

x_elec = 0.036    # x, y, and z dimensions are measured from our Fusion 360 model
z_elec = 0.060

y_elec = 0.025658279
y_elec_funky = 0.7 * y_elec

v_elecs = x_elec * z_elec * y_elec_funky
v_elec_hole = (x_elec) * (z_elec) * (y_elec)
v_ep_elec = v_elec_hole - v_elecs

# this next section is to determine the max radius for the excess cone, the void
# space below the syntactic foam and potted electronics
# Length internal you have to get from a CAD file

length_internal = .088175
max_depth_xs = length_internal - z_elec
max_r_xs = max_depth_xs * tan(0.6649704)
print(max_r_xs)

### Volumes ###
# This section is for volume calcs of the EDR


v_edr_shell = 0.00014694
v_whole_edr = v_edr_shell + .000304 + .00001442

r_xs = max_r_xs
#r_xs = 0.019

v_foam_cyl = pi * (0.04445)**2 * 0.03070478
v_foam_cone = pi * (1 / 3) * (0.04445)**2 * (0.04445) / tan(0.6649704)
#the length of the cone is opposite, the radius is adjacent

v_xs_cone = pi * (1 / 3) * (r_xs)**2 * ((r_xs) / tan(0.6649704))
v_foam = v_foam_cyl + v_foam_cone - v_xs_cone - v_elec_hole

v_fill_bottom = v_whole_edr - (v_foam + v_edr_shell + v_elec_hole)

print("The volume of the whole EDR is ", v_whole_edr)
print("The volume of the shell is ", v_edr_shell)
print("The volume of the foam is ", v_foam)
print("The volume of the hole in the foam is ", v_elec_hole)
print("The volume of what's left is ", v_fill_bottom)

# Densities in kg/m^3, the printers in Small can print Onyx,
# Windform GT is our target material
```

```
rho_pe = 1830
rho_onyx = 1190
rho_gt = 1190
rho_sw = 1027

rho_edr_target = 0.9 * rho_sw
rho_edr_target_2 = 0.8 *rho_sw

# Mass in kg

m_elecs = 0.053
# mass of the electronics measured in lab space

m_pe_elecs = rho_pe * v_ep_elec
m_shell = rho_gt * v_edr_shell

m_foam_p_hi = rho_p_1 * v_foam
m_foam_p_lo = rho_p_3 * v_foam

m_buoy = v_whole_edr * rho_edr_target # bouyancy from Archimedes
Principle, this is our max mass
print(m_buoy)


m_left_p_lo =  m_buoy - m_elecs - m_pe_elecs - m_shell - m_foam_p_hi
m_left_p_hi =  m_buoy - m_elecs - m_pe_elecs - m_shell - m_foam_p_lo

print("If we use the prism of foam, our excess mass
is between ", m_left_p_lo, " and ", m_left_p_hi)

print((m_left_p_hi + m_left_p_lo )/2 / v_fill_bottom)
print(m_pe_elecs)
print((m_elecs + m_pe_elecs)/v_elec_hole)

# How much tungsten can we use
# Tungsten will be in the potting epoxy

rho_W = 19600 #tungsetn's symbol is W,
https://www.engineeringtoolbox.com/metal
-alloys-densities-d_50.html

m_all_W = v_fill_bottom * rho_W

m_all_pe = v_fill_bottom * rho_pe

print(m_all_W, " if we use just tungsten, ", m_all_pe,
" if we just use epoxy.")

# Getting the exact value for coeff_w
```

```
x = Symbol('x')

b =  solve( x * (v_fill_bottom * rho_W) + (1 - x) *
(v_fill_bottom * rho_pe) - m_left_p_lo, x)
print(b, " is the proportion by volume of W to Epoxy,
if we use the prism foam")

# Python3 program to convert a list
# of integers into a single integer
def convert(list):

    # Converting integer list to string list
    # and joining the list using join()
    res = float("".join(map(str, list)))

    return res

b_f = convert(b)
vol_W = b_f * v_fill_bottom
vol_pe = (1 - b_f) * v_fill_bottom
m_W_p = vol_W * rho_W
m_pe_p = vol_pe * rho_pe

vol_ml_w = vol_W * 1000000
vol_ml_pe = vol_pe * 1000000

print("If we use the prism, we use ", m_W_p, " kg of
W and ", m_pe_p, " kg of epoxy")
print("So the mix is ", vol_ml_w, " mL of tungsten
and", vol_ml_pe, " mL of epoxy")
```

Bibliography

[1] Sailing Issues. Diederik Willemsen; [Oct 2, 2018; Oct 20, 2018].

[2] NASA. Glenn Research Center: Nancy Hall; [May 5, 2015; Sept 20, 2018].

[3] Agile 101. Agile Alliance. [2018; Nov 18, 2018]

[4] Windform - Technical Data Sheets. CRP Technology S.R.L. [2018; Nov 5, 2018]

[5] Thermoplastics Datasheets. Farnell. [2018; Nov 18, 2018]

[6] Windform GT. CRP Technology S.R.L. [2019; Mar 26, 2019]

[7] Windform SP. CRP Technology S.R.L. [2019, Mar 26, 2019]

[8] Windform High-Performing Features. CRP Technology S.R.L. [2019, Mar 26, 2019]

[9] Donglai Gong. Virginia Institute of Marine Science. [2018]